

1 ~~Using large-scale tracer-aided models to constrain ecohydrological partitioning in~~
2 ~~complex,~~Enhancing process interpretation with isotopes: potential discharge-isotope
3 trade-offs in ecohydrological modelling of heavily managed lowland catchments

4
5 Hanwu Zheng^{1,2*}, Doerthe Tetzlaff^{1,2,3}, Christian Birkel⁴, Songjun Wu¹, Tobias Sauter², Chris Soulsby^{3,1}

6
7 ¹Leibniz-Institute of Freshwater Ecology and Inland Fisheries, Berlin, Germany

8 ²Geography Institute and IRI THESys, Humboldt University of Berlin, Berlin, Germany

9 ³Northern Rivers Institute, School of Geosciences, University of Aberdeen, Aberdeen, UK

10 ⁴Department of Geography, University of Costa Rica, San Jose, Costa Rica

11 *Corresponding author: hanwu.zheng@igb-berlin.de

12
13 **Abstract**

14 Tracer-aided modelling (TAM) ~~enhance~~can help quantify ecohydrological ~~process~~
15 ~~understanding~~processes, as stable water isotopes ($\delta^{18}\text{O}$ and $\delta^2\text{H}$) can ~~help constrain equifinality~~
16 ~~and~~ provide complementary information beyond streamflow. ~~Despite being primarily applied~~
17 ~~in~~ and help constrain equifinality. Whilst TAM has been successfully undertaken in smaller
18 rural research (<100km²) catchments with ~~minimal disturbance, TAM may assess epistemic~~
19 ~~uncertainties from unrecorded human activities affecting streamflow, improving model~~
20 ~~reliability~~limited anthropogenic impacts, its utility in more heavily managed catchments
21 remains untested, particularly as isotope samples are usually unavailable. This study
22 investigated four sub-catchments (Berste, Wudritz, Vetschauer, and Dobra) in the heavily-
23 managed Middle Spree River basin (ca. 2800 km²), in NE Germany; ~~a~~ a strategically vital water
24 resource supplying drinking water to the capital of Berlin, Germany's capitalGermany, and
25 sustaining agricultural and industrial demands. ~~Detailed evaluation of~~Disentangling
26 ecohydrological water partitioning in this evapotranspiration (ET)-dominated region is

27 complicated by heterogeneous land use, extensive hydraulic infrastructure and ~~overall a long~~
28 legacy of intensive management. We used the spatially distributed tracer-aided model STARR
29 to simulate ~~the effects of natural~~ water fluxes and storage ~~flux~~ dynamics ~~and management~~
30 ~~interventions on streamflow~~ over a 6-year period. ~~Seasonal~~Temporally coarse (seasonal)
31 isotope data was used ~~for~~in calibration ~~additionally~~as well as streamflow to ~~streamflow~~
32 ~~effectively captured help constrain estimates of~~ subsurface runoff, ~~with isotope fractionation~~
33 ~~intensity strongly linked to ET apportionment. This multi-criteria calibration helped reduce~~
34 ~~equifinality in complex systems with human-induced epistemic challenges. Epistemic errors~~
35 ~~were manifested as strong trade-offs between the information content of the different~~
36 ~~calibration constraints (i.e., streamflow sources and ET partitioning. In most cases balanced~~
37 ~~calibrations using both isotopes). Although compromised solutions occasionally failed to meet~~
38 ~~acceptable performance thresholds for both calibrated variables, such conflicts highlight~~
39 ~~potentially important mismatches in~~ and discharge increased confidence in plausible process
40 representation, in the modelling. When the trade-offs between dual calibration targets could
41 not be reconciled, these were likely explained by anthropogenic factors that were not easily
42 incorporated in the modelling framework. Such trade-offs therefore provide opportunities for
43 learning about epistemic errors (e.g. un-represented water withdrawals for irrigation) that can
44 be used to improve future models for heavily managed catchments. Our modelling framework
45 shows the potential for informative insights from wider use of ~~(even sparse)~~ isotope data sets
46 in tracer-aided modelling of complex, heavily managed catchments.

47

48

49 **Highlights:**

50 **1. runoff generation processes.**

51 ~~2.1. Ignoring minor evaporation~~ Seasonal isotopes are valuable model constraints in

52 ~~modelling biases ET partitioning, managed catchments~~

53 ~~3.2. Streamflow & Sparse seasonal~~ isotope do not constrain spatial ET

54 ~~distribution, data may underestimate fractionation~~

55 ~~4.3. Streamflow-isotope trade-offs indicate epistemic errors in~~

56 ~~observations~~ uncertainties related to management.

57 ~~Catchments without historical mining effects exhibit large groundwater discharge.~~

58

59

60 1. Introduction

61 Characterizing ecohydrological processes in sparsely monitored catchments with
62 heterogeneous landscapes is inherently challenging due to spatially variable flow pathways and
63 non-stationarity in climate rainfall inputs (Hrachowitz et al., 2013; McDonnell et al., 2007).
64 This challenge can be even greater in catchments heavily modified by human activities, where
65 a long and on-going history of disturbance can fundamentally alter processes and functioning
66 (Marx et al., 2021). Distributed hydrological models are useful tools in addressing these
67 challenges and are capable of capturing the dominant processes across spatio-temporal scales
68 through regional parameterization (Fatichi et al., 2016). However, increasing model
69 complexity to capture catchment heterogeneity makes it difficult to identify when models give
70 “*the right answer for the wrong reason*” (Kirchner, 2006). In most catchments, rainfall and
71 streamflow are the only available data for modelling. Streamflow-based calibration has
72 therefore been the standard approach in hydrological modelling, leveraging the widespread
73 availability of river discharge data to estimate model parameters across diverse catchments
74 (Hrachowitz et al., 2013). However, calibration based on streamflow observations (single or
75 multiple gauges) alone are usually insufficient to constrain hydrological model uncertainty, as
76 certain parameters remain non-identifiable (Herrera et al., 2022). Consequently, simulations
77 with multiple parameter sets can give equally plausible outputs, with process equifinality being
78 a pervasive issue in model applications (Beven, 2006). Multi-criteria calibration, ~~that is,~~
79 leveraging complementary datasets (e.g., soil moisture, ET, groundwater) in addition to
80 streamflow, to mitigate this effect is increasingly common (He et al., 2019; Kuppel et al., 2018;
81 Oliveira et al., 2021; Shah et al., 2021; Wu et al., 2023). However, classical hydrometric
82 observations alone usually do not contain sufficient information to calibrate models and other
83 observations such as isotopes are needed to improve understandings of storage and flux
84 dynamics in catchments (Schilling et al., 2019).

85

86 Stable water isotopes ($\delta^{18}\text{O}$, $\delta^2\text{H}$) are ~~a potential solution~~proven tools that can help identify
87 water sources, flow paths, and transit times, thus revealing process-~~heterogeneity-based~~
88 function in catchments (Holmes et al., 2023; Klaus and McDonnell, 2013; Sprenger et al.,
89 2015). They are ~~often~~increasingly used as complementary datasets to streamflow, offering
90 additional insights into catchment hydrological behavior that can aid model parametrization
91 and modellingcalibration (Fenicia et al., 2008). In many cases, the integration of isotopes into
92 ~~model~~the modelling process has advanced process representation, improving understandings
93 of water partitioning and storage-flux interactions in heterogeneous landscapes (Birkel and
94 Soulsby, 2015; Luo et al., 2024; McDonnell and Beven, 2014; Smith et al., 2022).
95 Consequently, tracer-aided models (TAMs) have been increasingly applied worldwide (Jung
96 et al., 2025). ~~However, many~~

97

98 Almost all TAM studies ~~showed~~show inevitable trade-offs in model performance resulting
99 from conflicting information in the streamflow and isotopes ~~data~~timeseries (Birkel et al., 2015;
100 Scudeler et al., 2016; Wu et al., 2023). Such differences can highlight errors in model structure
101 and inappropriate process conceptualization (Beven, 2006; McDonnell et al., 2007; Wu et al.,
102 2025). ~~This is sometimes inevitable, such as when unknown anthropogenic influences affect~~
103 ~~hydrological behaviour. For example, unregulated water abstractions and artificial drainage~~
104 ~~can alter streamflow patterns, but simulations may still reproduce observed discharge, even~~
105 ~~without parameterising human effects into models via overfitting, which can result in a~~
106 ~~misleading representation of the system.~~ In addition, using some observations as “soft data”
107 (i.e. qualitative information or measured data that are not used in calibration) to constrain
108 models can alleviate some of the above issues (Efstratiadis et al., 2010; Wu et al., 2023).
109 However, failing to rigorously evaluate trade-offs between isotopes and streamflow in

110 calibration risks producing structurally biased results, even if models achieve seemingly
111 acceptable objective metrics for both datasets. Explorations of how these trade-offs in multi-
112 criteria modelling using isotopes to help better understand hydrological processes and
113 indicating further improve models are relatively rare.

114

115 Most TAMs focus on rural catchments (e.g. Soulsby et al., 2015) with limited anthropogenic
116 disturbance (Yang et al., 2023), while complexities of ecohydrological processes are
117 exacerbated in human-dominated systems where management measures can fundamentally
118 alter hydrological connectivity and function (Wada et al., 2017). This creates critical unknowns
119 in characterizing hydrological processes under anthropogenic alterationsimpacts. In this regard,
120 advancing tracer-aided methods to systematically evaluate hydrological dynamics at different
121 spatial and temporal scales in heavily managed catchments can ~~have advantages in help~~
122 improve modelling (Smith et al., 2021).

123

124 In this study, water stable isotopes ($\delta^{18}\text{O}$ and $\delta^2\text{H}$) were used in a tracer-aided hydrological
125 model (Spatially distributed Tracer-Aided Rainfall-Runoff, STARR), to help constrain
126 estimates of ecohydrological partitioning and water balance compartments in four heavily
127 modified sub-catchments of the Middle Spree catchment (MSC) in eastern Germany. These
128 include the effects of agricultural irrigation, land use change, urbanisation and historic lignite
129 mining with associated groundwater pumping- to de-water coal seams. The area impacts a
130 major national water resource, as the Spree river forms Berlin's water supply and ongoing
131 pressures and intensifying climate change have the potential to threaten future water provision
132 and ecosystem stability (Arndt and Heiland, 2024). Despite this significance, quantitative
133 evaluation of ecohydrological processes in the MSC is currently limited, as records of intensive
134 water use are not always available, historic impacts are often undocumented and parameterising

135 these human influences in hydrological models are difficult. Therefore, this study aims to
136 integrate streamflow and isotope calibration targets to provide a preliminary insight ~~of~~into
137 ecohydrological couplings between storage and fluxes, as well as effects on the partitioning
138 into runoff generation processes and ET fluxes in parts of the MSC, ~~with~~. The study had the
139 following specific objectives ~~addressed~~:

- 140 1. ~~Assessing trade-offs between~~ To assess the additional values of using seasonally-
141 sampled isotopes in streamflow and isotope-aided constraints in calibration of
142 ecohydrological modelling in intensively addition to discharge in the simulation of
143 heavily managed ~~lowland~~ catchments.
- 144 ~~2. Quantifying the spatio-temporal dynamics of the water balance in intensively managed~~
145 ~~lowland catchments during wet and dry periods.~~
- 146 2. To evaluate the contribution of isotopes in improving estimates of water flux
147 partitioning and identifying the potential influence of unknown human management
148 impacts.
- 149 3. Examining how management activities can bias ecohydrological models and advancing
150 isotope-aided methods to disentangle process dynamics in human-dominated systems.

151 2 Materials and Methods

152 2.1 Study catchment

153 The Mid-Spree catchment (MSC) is located in the SE (Southeast) of Brandenburg, Germany
154 (Figure 1). The 2806 km² sub-basin forms the middle part of the much larger Spree catchment
155 (10105 km²), accounting for 28.6% of the entire catchment area. Within the MSC, the Spree
156 River flows from Cottbus to Beeskow and through the Spreewald UNESCO Biosphere Reserve,
157 which is an extensive wetland area. Climate is sub-continental with low precipitation and hot
158 and dry summers (Pusch et al., 2009). Mean annual precipitation in the headwaters of the entire
159 Spree catchment range from 600mm to 1000mm, decreasing to 556 mm in the MSC, making
160 it one of the driest regions in Germany. Average monthly temperatures range between 19.3°C
161 in summer (June to August) and 1.9°C in winter (December to February), respectively. Annual
162 potential evapotranspiration, based on the FAO-56 Penman-Monteith equation (Deutscher
163 Wetterdienst (DWD), 2024), reaches 726mm, making the MSC water-limited and highly
164 susceptible to climate change.

165

166 The topography is flat and 80% of MSC varies between 42 to 78 m.a.s.l. (meters above sea
167 level), though the maximum elevation is 155.6 m.a.s.l. The course of Spree River through the
168 MSC has a very low gradient (0.027 %).

169

170 We selected four gauged sub-catchments in the MSC: the river Berste (gauged at Bruckendorf),
171 the Wudritz catchment (gauged at Ragow), the Vetschauer Mill Creek (gauged at Vetschau),
172 and the Dobra catchment (gauged at Boblitz), in the southern tributaries of the Spree River as
173 the main study catchments (Figure 1). They are mostly dominated by farming, particularly
174 croplands (encompassing some of the most extensiveintensive farming areas in the MSC), with

175 pasture and coniferous forests forming the other two major land uses in the four sub-catchments,
176 accounting for 12-20% and 18-30% of the total area, respectively.

177

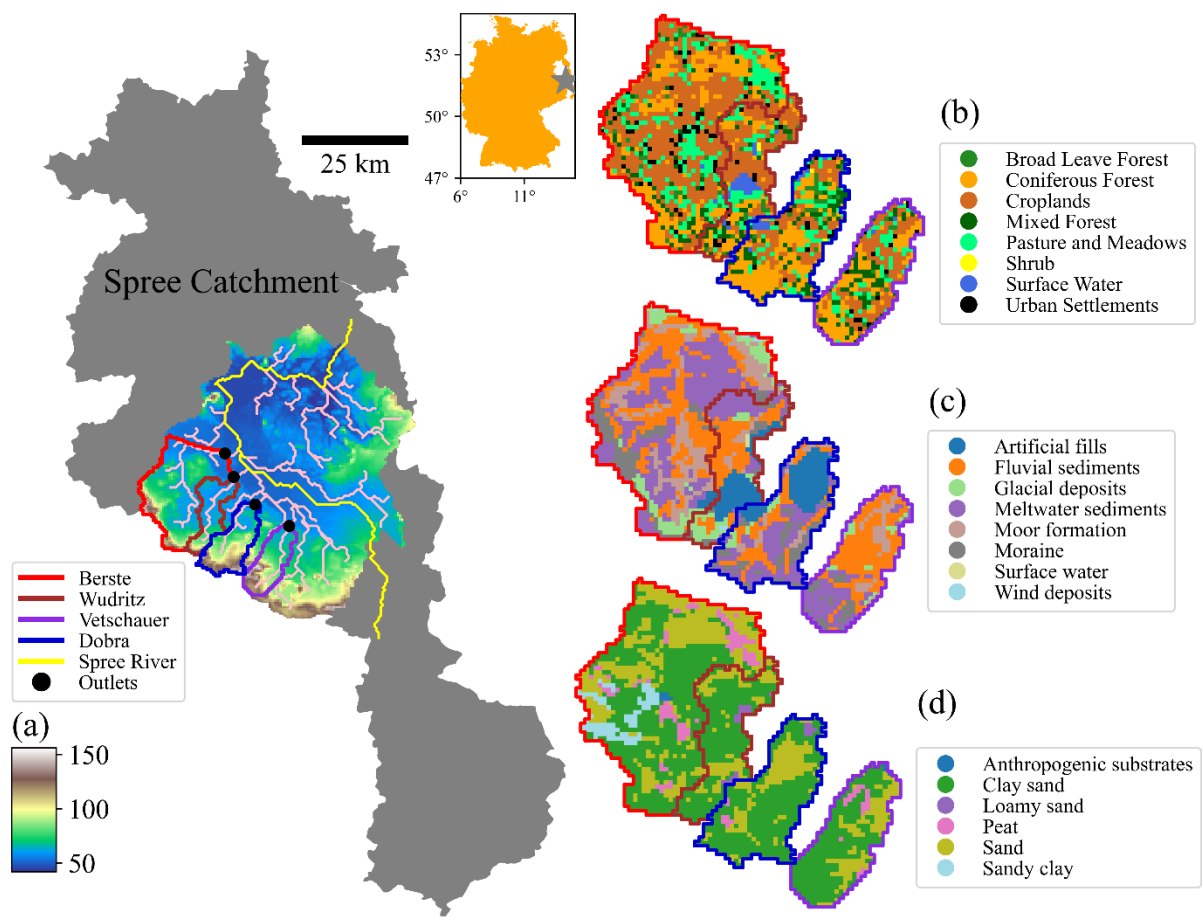
178 The geology of the sub-catchments is dominated by fluvial and meltwater sediments, especially
179 along the river reaches, while artificial fills (from mining spoil) constitute a major part ~~in~~of
180 the Wudlitz and Dobra catchments, as a result of historic lignite extraction (Landesregierung
181 Brandenburg, 2024). Sandy soils (58.7% of the area) and clay- sands (29.7%) dominate these
182 sub-catchments, while peat soils are sporadically distributed.

183

184 The four sub-catchments, like much of the MSC, were influenced by intense lignite mining
185 activities between 1960-1990 (Pusch and Hoffmann, 2000). ~~Of our study sites, the Wudritz and~~
186 ~~Dobra catchments were most severely affected, though lakes and restored areas now occupy~~
187 ~~the former mining areas. These lakes are relatively small, shallow and linked to streamflow in~~
188 ~~an unknown and non-stationary way.~~ Pumped mine water (sump water), from de-watering
189 former open-cast mines in the Altdoberm, Schlabendorf and Seese regions was discharged to
190 the southern tributaries of the Spree River. After the sharp decline in lignite production in the
191 early 1990s, discharge volumes from southern tributaries in the MSC to the Spreewald are
192 believed to be close to the pre-mining situation since 2018 (Landesregierung Brandenburg,
193 2024). However, more generally in the Spree catchment, the ~~decline of pumped sump water~~
194 ~~volumes has been faster than the replenishment of the groundwater deficit, and the~~ lowered
195 groundwater table leads now to a high risk of lower river flows and water shortages in the MSC,
196 and constitutes a threat to Berlin's water supply further downstream (Arndt and Heiland, 2024).
197 At present, ~~in these four sub-catchments,~~ drinking water in the studied region is extracted from
198 groundwater wells, ~~while authorised.~~ Agricultural and industrial water withdrawals are not
199 permitted in ~~channel~~the Vetschauer and Dobra catchments, while this extraction from the

200 surface water for agriculture irrigation are limited to spring and summer months (at the Berste
 201 and upstream area of the Wudritz catchment. The Wudritz and Dobra catchments were most
 202 severely affected by historic mining activities several decades ago, and some parts of the mined
 203 areas have been converted into small lakes, with the Wudritz catchment having the largest
 204 surface water area among the four catchments. (Table 1)(Landesregierung Brandenburg, 2024).

205
206
207



208
209
210
211

Figure 1. (a) Elevation, river network and catchment borders, (b) land use, (c) geology, and (d) soil types of the four sub-catchments in the MSC.

212 *Table 1. Catchment characteristics of the MSC and its sub-catchments (Berste, Wudritz,*
 213 *Dobra, Vetschauer)*

Land use (%)	MSC	Berste	Wudritz	Dobra	Vetschauer
Area (km²)	2806.3	316	101.3	131.8	107.8
Land use (%)					
Urban settlements	5.5	5.2	3.5	3.0	4.2
Surface water	2.9	0.2	7.7	3.0	0.7
Pasture and meadows	19.2	17.2	12.3	13.7	13.7
Croplands	30.6	48.4	44.9	25.6	33.9
Shrub	0.8	0	0.5	0.4	0.2
Coniferous forest	29.7	20.6	18.5	36.6	30.4
Mixed forest	8.5	6.5	8.1	12.0	14.1
Broad leaf forest	2.8	1.9	4.5	5.7	2.8
Geology (%)					
Artificial fills	4.7	1.0	23.7	24.1	0
Fluvial sediments	25.7	27.7	29.9	20.5	49.4
Glacial deposits	9.3	8.2	11.4	3.2	5.6
Meltwater sediments	28.0	35.0	21.0	29.8	23.7
Moor formation	17.3	18.1	5.2	5.7	12.5
Moraine	12.2	9.5	8.6	16.7	8.8
Wind deposits	2.8	0.5	0.5	0	0
Soil (%)					
Peat	8.5	7.3	0	1.5	5.1
Clay sand	29.7	51.4	70.9	71.0	66.6
Sand	58.7	34.1	24.9	26.2	27.4
Clay	0.6	0	0	0	0
Sandy clay	1.1	6.8	0	0	0
Anthropogenic substrates	1.1	0.4	0	0	0.9
Loamy sand	0.3	0	4.2	1.3	0
Area (km²)	2806.3	316	101.3	131.8	107.8

214

215 **2.2 The STARR model and adaptations to simulate low-relief and different land use**

216 The spatially distributed tracer-aided rainfall-runoff (STARR) model (van Huijgevoort et al.,
 217 2016) integrates the general conceptual structure of the HBV-light hydrological model
 218 (Lindström et al., 1997; Seibert and Vis, 2012) in a distributed, gridded framework that enables
 219 flux tracking of water and tracers through catchments. It is operated in the PCRaster Python
 220 framework (Karssenberget al., 2010). The STARR model includes a module for tracking of
 221 stable water isotopes and tracer mixing (van Huijgevoort et al., 2016; Ala-aho et al., 2017). As
 222 a fully distributed model, hydrological fluxes are simulated in each grid cell based on a simple
 223 reservoir structure and water balance equations (Figure S1). ~~This~~The canopy, soil and

224 groundwater storages are each conceptualised as a single layer, with throughfall, seepage and
225 capillary flux serving as the flow paths connecting them. The model has been successfully
226 applied in TAMs across a range of catchments at multiple scales (0.2-2500 km²) in contrasting
227 environments (Ala-Aho et al., 2017; Correa et al., 2020). The basic hydrological components
228 and a brief summary of the STARR model are given in the supplementary materials (Appendix
229 A), while van Huijgevoort et al., (2016) and (Dehaspe et al., 2018) provide more detailed
230 descriptions.

231

232 Some of the assumptions of the STARR model, which was originally developed for
233 mountainous catchments and subsequently adapted for tropical and cold regions, are not
234 applicable in the lowland catchments studied here (the detailed equations used in modified
235 STARR model are shown in Table S1). TheFor example, a topographical wetness index was
236 not used to separate hillslope and lowland areas for runoff generation as in previous
237 applications. Further, runoff routing was determined by the Manning equation (Chow, 1959),
238 rather than assigning a pre-defined velocity.

239

240 Further, fractionation of stable water isotopes by evaporation in soil and interception storage
241 was adapted to follow the Craig-Gordon model (Craig and Gordon, 1965), rather than being
242 simulated by empirical representations (as in van Huijgevoort et al., 2016, Correa et al., 2020).
243 The partitioning of evapotranspiration (ET) in the original STARR model was not applicable
244 in the MSC as the isotopic composition of evaporation was sometimes more enriched than
245 calculated isotopes of ambient atmospheric vapour (Chakraborty et al., 2018). Therefore, the
246 partitioning method from HYDRUS-1D (Simunek et al., 2013) was used here, where the
247 transpiration originates from, and is linearly related to, soil and groundwater saturation. In
248 order to keep parameter consistency, we adapted the interception module to the one developed

249 in the HYDRUS-1D and the EcoPlot models (Stevenson et al., 2023), with the interception
250 volume and the maximum capacity being controlled by LAI. Channel grid cells were distinct
251 in representing different runoff and routing processes. Roughness (Manning coefficient) used
252 in the kinematic wave equation was defined as 0.025 in the channel grid cells as recommended
253 in Chow (1959), while other non-channel grid cells were assigned the values similar to van der
254 Sande et al., (2003) and according to the land use (Table S2). The channel width used in the
255 kinematic wave equation was estimated from recent Google earth maps (03.08.2024), while
256 the width for non-channel grid cells was defined as the grid cell size (i.e., 500 m). Other
257 parameters were the same for all grids. Explicit parameterization of anthropogenic factors (i.e.,
258 ~~major water withdrawn~~withdrawals in the Berste, and upper Wudritz, operation of restored lakes
259 in Wudritz and Dobra) was excluded due to insufficient data, ~~and the~~ though the modelling
260 results allowed these influences ~~will to~~ be ~~evaluated~~hypothesized.

261

262 **2.3 Data Acquisition**

263 2.3.1 Forcing Datasets

264 The spatial resolution of the model grid was defined at 500 m as a trade-off between adequate
265 spatial detail and computation time (Smith et al., 2021). All datasets listed in Table 2 were
266 downscaled or upscaled to the same resolution for consistency.

267

268 The meteorological inputs were acquired from twenty weather stations in or near the study
269 catchments (i.e., measuring precipitation (P), temperature (T), relative humidity (RH)) and grid
270 products of potential evapotranspiration (PET) operated by the German Weather Service
271 (DWD) were used, and the station datasets were linearly interpolated to spatially distributed
272 (500 m) inputs. The 8-day composite LAI dataset at 500 m resolution (MCD15A3H V6.1) was
273 used to characterise LAI dynamics. The dataset was accessed through Google Earth Engine

274 (GEE). The cloud masking process was based on GEE and linear resampling at daily resolution
275 was conducted, corresponding to the other input datasets. A global product to estimate the
276 stable water isotopic composition (Interannual Monthly Mean values) of rainfall from (Bowen
277 and Revenaugh, 2003 et al., 2005) was used and set as daily rainfall isotope input to the model
278 constant in each month and equal to the monthly product value. This monthly value showed a
279 consistent seasonal pattern with measurements from a rainfall station (daily resolution and
280 aggregated to monthly values) downstream of the study area (Demnitzer Millcreek Catchment
281 (DMC); 52°23'N, 14°15'E; Landgraf et al., 2022), indicating the representativeness of the
282 modelled rainfall isotope input (Figure S2).

283

284 2.3.2 Datasets for model calibration and evaluation

285 Daily discharge from 2018 to 2023 and seasonal streamwater isotope data were collected
286 during 2021-2023 in the outlets of the four catchments at the Bruckendorf (Berste), Ragow
287 (Wudritz), Boblitz (Dobra), and Vetschau (Vetschauer mill creek). (Landesregierung
288 Brandenburg, 2024). Gauging stations (Figure 1) were used for model calibration (Table 2).

289

290 Stable isotopes were sampled (via instantaneously collected “grab” sampling) every season
291 over three years (2021, 2022, 2023) at the river outlet of the four catchments, and we used
292 cavity ringdown spectroscopy (Picarro L-2130i, Picarro Inc, CA, USA) to analyse the ratio of
293 the heavy stable isotopes of oxygen (¹⁸O) and hydrogen (²H) relative to the Vienna Standard
294 Mean Ocean (VSMOW) (for detailed sampling and pre-process procedure refer to Chen et al.
295 (2023)).

296

297 Further, the MODIS ET (MOD16A2GF from GEE) and PML ET (Zhang et al., 2019) 8-day
298 composite products were compared with simulation results to evaluate evapotranspiration

299 ~~simulation~~simulations, and qualitatively check the model performance. Despite uncertainties,
 300 the PML product aligned better with flux tower (51.8922 N, 14.0337 E) records in the
 301 Spreewald (Table 2) indicating its usefulness as a comparator for modelling results (Figure
 302 ~~S2~~S3). Groundwater (GW) levels from 3 wells distributed in the studied region were collected
 303 (Landesregierung Brandenburg, 2024) and the annually varying pattern of each well were used
 304 to further identify the robustness of the model.
 305

306 *Table 2. Overview of the datasets used in this study*

Forcing datasets	Temporal resolution and period	Spatial resolution
P, T, RH	Daily; Jan 2014 - Dec 2023	20 stations
PET	Daily; Jan 2014 - Dec 2023	1 km × 1 km cells
Discharge	Daily; Jan 2014 - Dec 2023	4 stations
Rainfall isotopes	Monthly; Jan 2014 - Dec 2023	5 × 5 arc minutes
LAI	8 days; Jan 2014 - Dec 2023	500 m × 500 m cells
Calibration datasets		
Discharge	Daily; Jan 2014 - Dec 2023	4 stations
Streamwater isotopes	Seasonally; Jan 2021 - Dec 2023	4 sample locations
Evaluation datasets		
PML ET	8 days; Jan 2014 - Dec 2023	500 m × 500 m cells
MODIS ET	8 days; Jan 2014 - Dec 2023	500 m × 500 m cells
FLUXNET	Daily; Jan 2011 - Dec 2014	1 station in the Spreewald
<u>GW level</u>	<u>Weekly; 2019-2023</u>	<u>3 stations</u>

307

308

309 **2.4 Model parameterisation, sensitivity analysis and calibration**

310 2.4.1 Model parameterisation

311 The number of calibrated model parameters was minimised and therefore some of the
 312 parameters were assigned fixed values (Table S2). In total, 35 parameters were included for
 313 calibration and the assigned ranges for calibration were mostly adapted from previous
 314 applications of the STARR model, with some adjustments appropriate to the characteristics of
 315 the study catchments (Table S2). Parameters representing soil characteristics were distributed
 316 according to land use types (i.e., urban, water, pasture, cropland, shrub, forest) given the close

317 correlation between land cover and soil type in the region (see (Smith et al., 2021)). The ~~flux~~
318 ~~processes~~fluxes from interception to soil storage (throughfall and stemflow) are different
319 ~~in~~under forest and non-forest land use, as contrasting canopy characteristics affect the rainfall
320 partitioning (Guevara-Escobar et al., 2007), and the corresponding parameters were determined
321 separately.

322

323 2.4.2 Sensitivity analysis (SA)

324 We employed the Morris Method (Morris, 1991) to identify the most sensitive parameters. The
325 calculation used the SAFE tool (Sensitivity Analysis for Everybody, Pianosi et al., 2015). The
326 elementary effects (reflecting the sensitivity of each parameter) were calculated through
327 perturbing the starting parameter by a certain variation based on a radial one-at-a-time strategy.
328 ~~Nash-Sutcliffe Efficiency (NSE) (Hodson, 2022)~~Kling-Gupta efficiency (KGE) (Gupta et al.,
329 2009) of simulated streamflow or ~~streamwater~~stream water isotopes, corresponding to
330 calibration scheme, was used as the objective function in calculating the elementary effects
331 (Table 3). The Latin-Hypercube sampling method (Pianosi et al., 2015) was selected to
332 determine the starting parameter and following perturbation. The mean elementary effect of
333 each parameter was used to indicate the sensitivity of the corresponding parameters. Parameters
334 related to pastures, croplands, and forests were more sensitive than others, as they cover
335 majority of the catchment area (Table 4), and the estimated ecohydrological fluxes are mainly
336 shown for these three land uses.

337

338 2.4.3 Model calibration

339 The modified STARR model was run at daily time steps for the period from 2014 to 2023. A
340 4-year spin-up period (2014-2017) was applied, and the remaining six years were used for
341 calibration. The multi-objective non-dominated sorting genetic optimization algorithm II

342 (NSGA-II) (Blank and Deb, 2020; Deb et al., 2002) was applied to derive the Pareto-optimal
343 solutions. Five distinct calibration schemes were conducted based on measurements (i.e.,
344 streamflow and/or stream isotopes) at the outlet of the four catchments and are detailed in Table
345 3. The first scheme (discharge-only based calibration) was calibrated only on the streamflow
346 of all four catchments (multi-gauged streamflow calibration) using the NSEKGE values of
347 simulated streamflow as the objective function. Considering the potential for heterogeneity in
348 the hydrological functioning of each catchment and to assess the additional information content
349 of the isotope data in the modelling, calibrations (the other four schemes as in Table 3) were
350 also carried out in each catchment independently (Scheme 2: Berste; Scheme 3: Wudritz;
351 Scheme 4: Vetschauer; Scheme 5: Dobra) and based on NSEKGE values of simulated
352 streamflow and isotope (isotope-aided calibrations) (Table 3). Simulations based on NSGA-II
353 were conducted with 4080 generations and 200280 individuals in the population per generation,
354 and the first pareto front in the 40th80th generation were employed as the solution. Five
355 independent calibrations were conducted for each calibration scheme to minimize potential
356 biases. Balanced, discharge-dominated, and isotope-dominated solutions were defined in the
357 isotope-aided calibrations (schemes 2-5), five parameter sets from each of the five independent
358 calibrations (25 parameter sets in total) were selected for each of these three solution types.
359 These three solution types corresponded to parameter sets in the middle (with minimum
360 Euclidean distance to the best KGE of discharge and isotopes, i.e., (KGE_discharge=1.0,
361 KGE_isotope=1.0)) and the edges of the Pareto front, respectively. In the scheme 1, only
362 balanced solutions (minimum Euclidean distance to the best KGE point, i.e., KGE_Berste=1.0,
363 KGE_Wudriz=1.0, KGE_Vetschauer=1.0, KGE_Dobra=1.0) were employed. The aggregated
364 25 parameter sets for each solution type (i.e., balanced, discharge-dominated, isotope-
365 dominated) encompass a broad range of parameter variability and allow a robust comparison
366 among solution types. No validation period was employed, as the present study attempted aimed

367 to better constrain ecohydrological processes in the MSC, rather than for forecasting
 368 applications. ~~Further, Also, others have argued that~~ calibrating to the full available data and
 369 skipping model validation ~~has been found~~ can be more robust than the traditional split-sample
 370 approach in hydrological modelling (Shen et al., 2022).

371

372 *Table 3. Five calibration schemes based on measured streamflow and isotope at the outlet of*
 373 *the four catchments. Sensitivity analysis was conducted separately on isotope and discharge*
 374 *measures in schemes 2-5.*

Calibration scheme	Streamflow	Isotope	Objective function in SA
Scheme 1	Berste Wudritz Vetschauer Dobra		$\sum_i NSE_i + \sum_i KGE_i$, i includes streamflow in all sub-catchments used in the scheme
Scheme 2	Berste	Berste	$NSE_{streamflow} KGE_{streamflow}$ or $NSE_{isotope} KGE_{isotope}$
Scheme 3	Wudritz	Wudritz	$NSE_{streamflow} KGE_{streamflow}$ or $NSE_{isotope} KGE_{isotope}$
Scheme 4	Vetschauer	Vetschauer	$NSE_{streamflow} KGE_{streamflow}$ or $NSE_{isotope} KGE_{isotope}$
Scheme 5	Dobra	Dobra	$NSE_{streamflow} KGE_{streamflow}$ or $NSE_{isotope} KGE_{isotope}$

375

376 **3 Results**

377 **3.1 Model performance**

378 3.1.1 Discharge simulations

379

380 *Table 4. The 6 most sensitive parameters in each calibration scheme. Subscript p, c, f represent*
 381 *pasture, croplands, forest, respectively. kS , kG LP, INT- α , K control processes of runoff from*
 382 *soil, runoff from groundwater, Actual ET, interception and ET partitioning, respectively; and*
 383 *FC is the soil water storage capacity.*

Scheme1	Scheme2	Scheme3	Scheme4	Scheme5
Discharge	isotope	discharge	isotope	discharge
kS_f	kS_e	kS_e	kS_e	kS_f
kS_e	K	kS_f	kS_f	K
kS_p	LP _e	kS_p	LP _e	kS_e
LP _f	FC _e	LP _e	FC _e	INT- α
LP _e	kS_f	FC _e	k	FC _e
FC _e	kG	INT- α	kS_p	INT- α

384

385

386

387

388

389

390

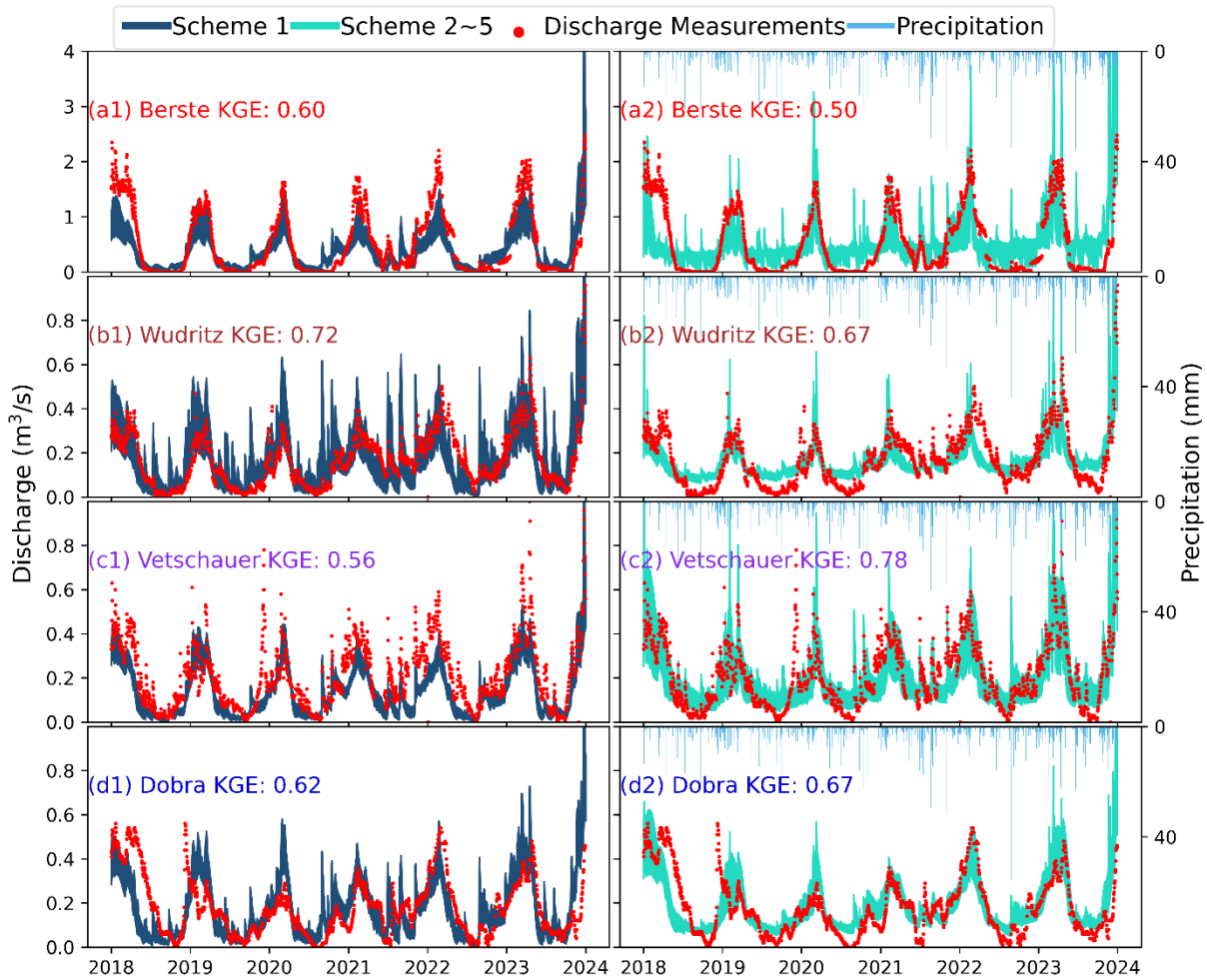
391

392

393

394

395



396

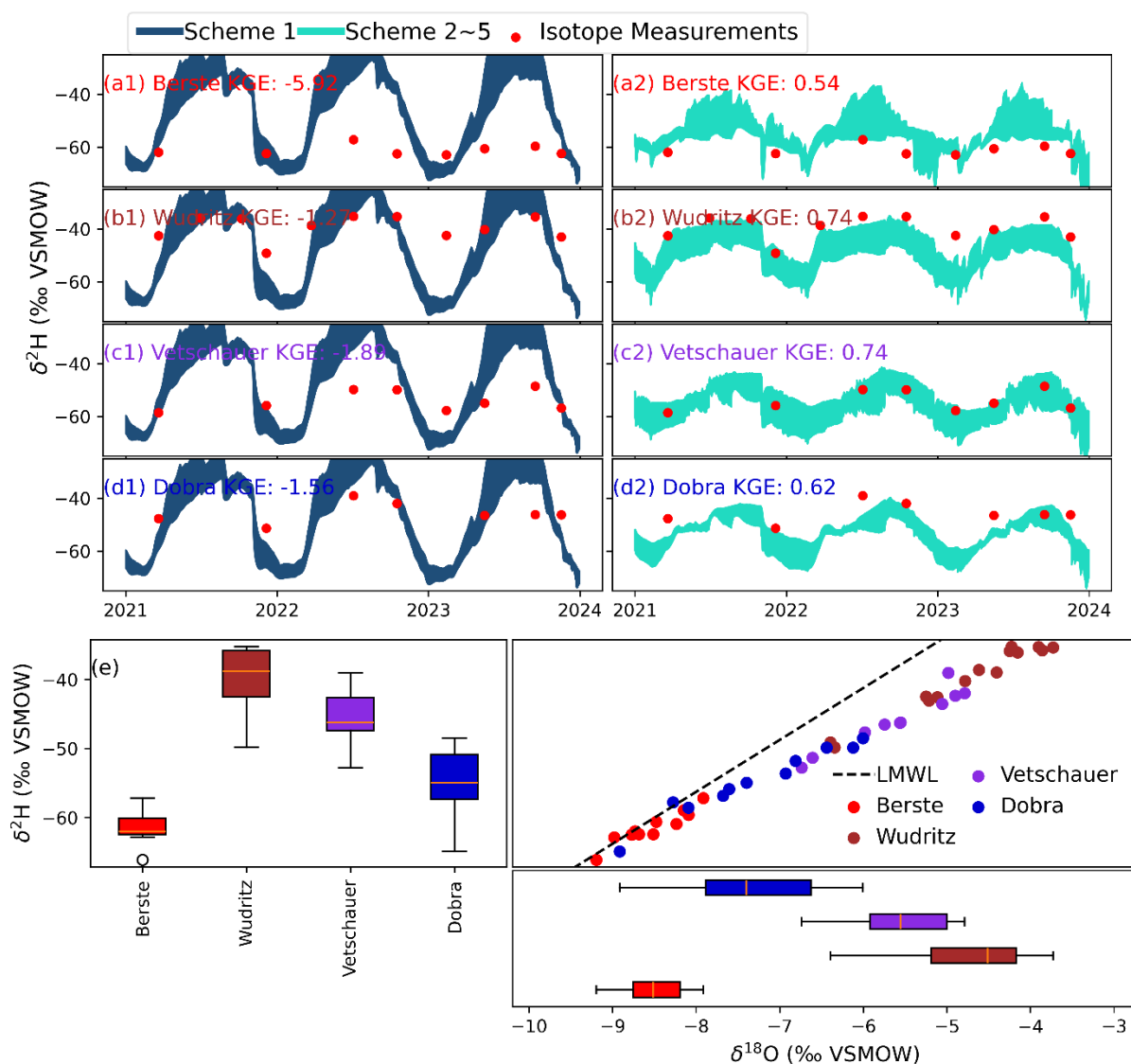
397 *Figure 2. Discharge simulations at the outlet of each catchment based on ~~each~~the balanced*
 398 *solutions in the calibration scheme- 1(first panel (a1, b1, c1, d1)) and schemes 2-5(second*
 399 *panel (a2, b2, c2 d2)). (a) Berste; (b) Wudritz; (c) Vetschauer; (d) Dobra. “BSI” and “BSS”*
 400 *are abbreviations for the simulation with Best Simulated Isotope and Best Simulated*
 401 *Streamflow, respectively.*

402

403 Discharge-only based calibrations (scheme 1) and ~~parameter sets with the best simulated~~
 404 ~~streamflow (BSS) in balanced solutions of the~~ isotope-aided calibrations (~~chemes~~schemes 2-5)
 405 successfully captured discharge dynamics in each catchment with average NSE (Figure 2)
 406 mostly KGE >0.6 (Table 5). ~~The uncertainty bands in scheme 1 were relatively large, but~~
 407 ~~bracketed the measurements for most of the time at most sites~~5 (Figure 2). The averaged NSE

408 ~~were slightly lower than BSS in schemes 2-5, suggesting~~ This performance was better
409 (KGE>~0.8) in discharge-dominated solutions of the isotope-aided calibrations (Figure S4).
410 Contrasting flow regimes were shown in each catchment, e.g., Berste presented low base flows
411 and Vetschauer had quicker responses to rainfall. Therefore, scheme 1 underestimated peak
412 flow, showing the trade-offs in balancing performance across the four ~~individual~~ catchments.
413 ~~However, variations in scheme 1 and BSS~~ Trade-offs between discharge and isotopes
414 objectives within each catchment (schemes 2-5) ~~generally underestimated peak flows and also~~
415 led overestimated base flows. ~~Parameter sets with the best simulated isotopes (BSI) in schemes~~
416 ~~2-5 gave large biases in modelled streamflow compared to measurements, showing much~~
417 ~~higher base flow, lower variations, and higher frequency of high flows,~~ flow (particularly in
418 Berste and Vetschauer where pronounced overland flow contributions were simulated (see
419 section 3.2.2): Wudritz) in the balanced solutions of schemes 2-5 (Figure 2).

420



424 *Figure 3. Isotope-Stream water isotope simulations at the outlet of each catchment based on*
 425 *each the balanced solutions in the calibration scheme: 1(first panel (a1, b1, c1, d1)) and*
 426 *schemes 2-5(second panel (a2, b2, c2 d2)).* (a) Berste; (b) Wudritz; (c) Vetschauer; (d) Dobra;
 427 *and (e) Dual isotope plots for streamwater isotopes from Jan 2021 to Dec 2023 in each*
 428 *catchment.*

430 The stream isotope signatures in the four catchments showed contrasting characteristics:
 431 (Figure 3). Overall, apart from the Berste, streamwater isotopes in each catchment plotted

432 below the local meteoric water line (LMWL), reflecting differences in fractionation processes.
433 The similar alignment of isotopes along a shared local evaporation line indicates comparable
434 atmospheric moisture demand among the catchments (Figure 3). The Berste exhibited the most
435 depleted isotopic signature ($\delta^2\text{H}$: $\sim -62\text{‰}$), while Wudritz was the most enriched catchment
436 ($\delta^2\text{H}$: $\sim -38\text{‰}$), and their enrichments positively correlated with the extent of surface water
437 area, although all catchments have low surface water coverage ($< 8\%$) (Figure 3). Simulations
438 in all solutions of each scheme 1 and BSS in schemes 2-5 reproduced the seasonal isotope
439 dynamics, with summer enrichment and winter depletion (Figure 3; Figure S5). However, the
440 variability of isotopes was overestimated in scheme 1 and in the discharge-dominated solutions
441 of schemes 2-5, although mean simulations and measurements were comparable and much
442 better performance were shown in the latter. This showed that different flow paths, mixing
443 processes and fractionation effects in the catchments were problematic likely unrealistic in the
444 discharge-only based calibrations (scheme 1) or BSS discharge-dominated solutions in isotope-
445 aided calibrations (schemes 2-5). ~~BSI~~ The balanced solutions or isotope-dominated solutions in
446 schemes 2-5 yielded much more consistent simulations of the isotope dynamics, although this
447 came at the cost of much poorer discharge performance (Figure 3). ~~The low NSE values~~
448 ~~between simulations and measures are because of the coarse temporal scale of samples and~~
449 ~~deviations in single sample point could result in large degradation in NSE values (Table 5);~~
450 Figure S5).

451

452

453

454

455

456

457
458
459
460
461
462
463
464
465
466

Table 5. NSE and KGE values for discharge and isotopes at different locations based on the different schemes. Values at multiple locations were only calculated in calibration scheme 1, while the metrics of the other four schemes (“schemes 2-5”) were given at corresponded calibrating outlets (i.e., values in Berste, Wudritz, Dobra and Vetschauer are from Schemes 2-5, respectively). The slash “/” separates results in the two ends of the pareto front, namely “BSS/BSI”.

Locations	Scheme 1				Schemes 2-5			
	Discharge		Isotope		Discharge		Isotope	
	NSE	KGE	NSE	KGE	NSE	KGE	NSE	KGE
Catchments								
Berste	0.69	0.57	-55.9	-3.93	0.74/ 18.8	0.66/ 4.03	-42.0/ 1.05	-3.84/0.57
Wudritz	0.77	0.83	-7.85	-0.76	0.82/ 0.06	0.85/0.24	-5.18/ 0.02	-0.99/0.68
Vetschauer	0.63	0.66	-2.48	-0.77	0.73/0.04	0.75/0.17	-1.44/0.96	-0.49/0.93
Dobra	0.46	0.69	-4.30	-0.56	0.62/ 0.36	0.56/0.02	-5.95/0.51	-0.89/0.66

467

3.2 Trade-offs between streamflow and isotope-based calibrations

3.2.1 Pareto front of simulations

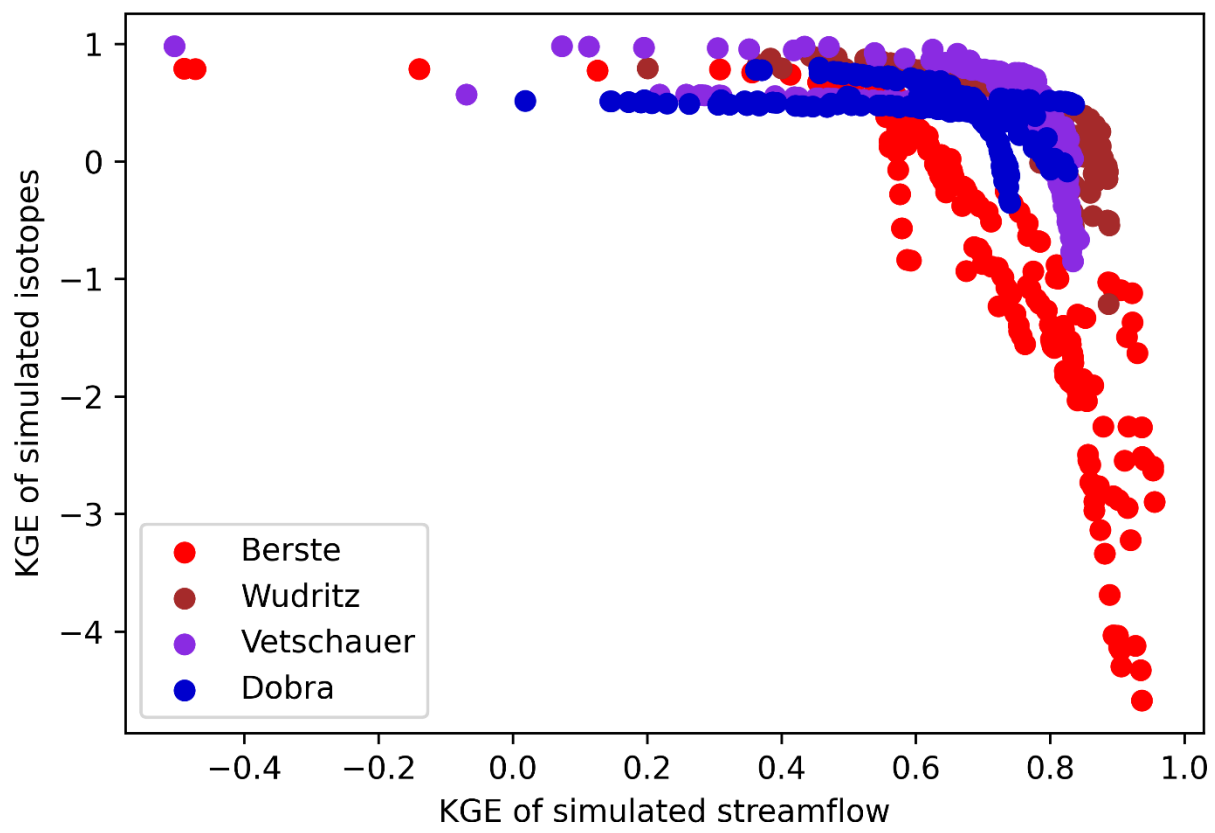
The Pareto ~~front~~fronts of simulations from schemes 2-5 show the range of potential solutions of streamflow and isotopes. ~~Points in the middle of the Pareto front represent the compromised~~ “trade-off” solutions based on both streamflow and isotopes (Figure 4). Berste resulted in lower ~~NSE or~~ KGE of both isotopes and streamflow than the other three catchments, while the ~~compromised~~balanced trade-off solutions in Vetschauer were the most satisfying, and its Pareto front was the narrowest ~~robust~~ (Figure 4). ~~The~~On each Pareto front, increased KGE of simulated discharge was accompanied by a slight decrease in the KGE of simulated isotopes, until the discharge KGE reached a certain threshold, beyond which the isotope KGE dropped

477

478 sharply. This threshold was approximately 0.7-0.8 at Wudritz, Vetschauer and Dobra, but only
479 around 0.5 at Berste. This ~~unsatisfactory solutions for performance at~~ Berste reflected the
480 stronger conflicting information provided by isotope and streamflow data under the existing
481 model structure and potentially reflected unknown ~~processes~~impacts resulting from ~~the intense~~
482 management. (see Discussion below).

483

484

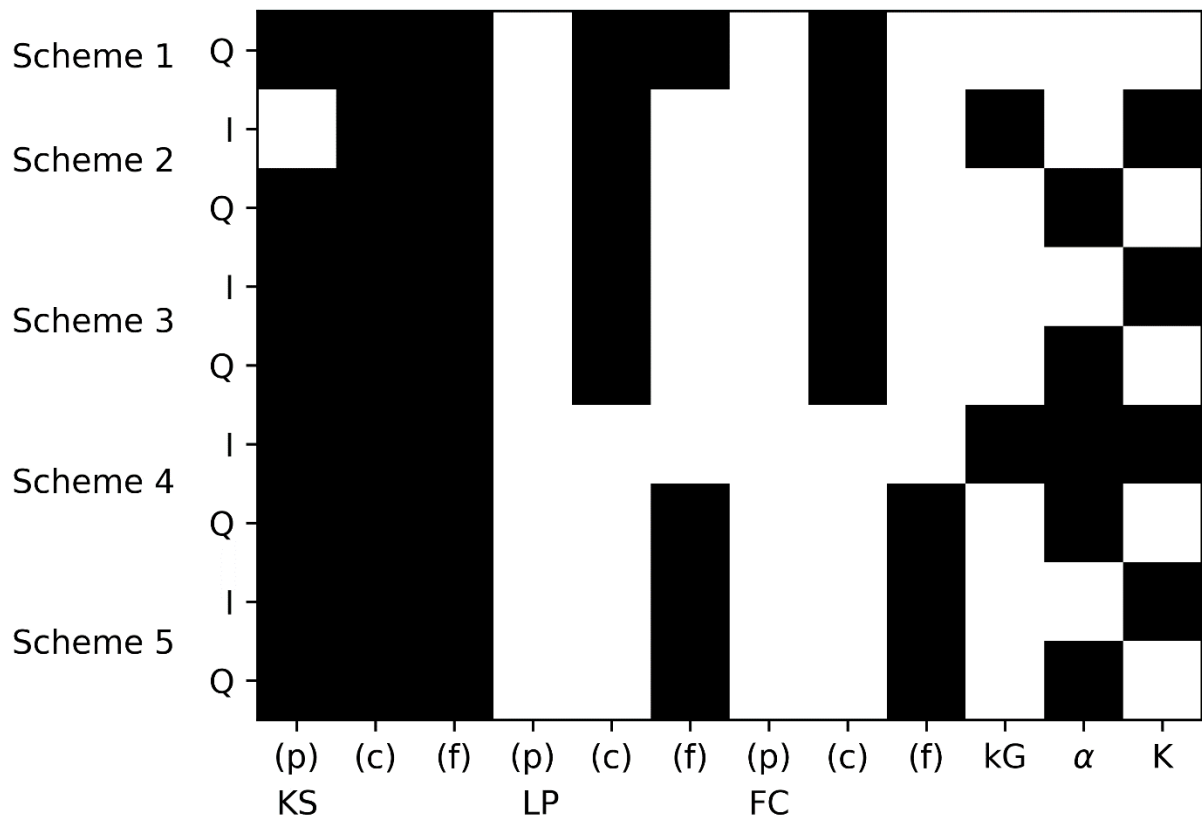


485

486 *Figure 4. Pareto ~~front~~fronts of simulations from all five independent calibrations in schemes*
487 *2-5. ~~Simulations on two ends of the front were excluded~~*

488

489



490

491 *Figure 5. Sensitive parameters in this plot. KGE of the compromised solutions in Berste,*
 492 *Wudritz, Vetschauer each calibration scheme (The top six sensitive parameters are shown*
 493 *shaded). I and Dobra can reach 0.14/0.23, 0.54/0.45, 0.62/0.75Q in the y-axis represent*
 494 *isotopes and 0.43/0.40 in streamflow/isotope discharge; (p), (c), (f) represent pasture,*
 495 *croplands, forest, respectively. kS, kG LP, α , K control processes of runoff from soil, runoff*
 496 *from groundwater, Actual ET, interception and ET partitioning, respectively; and FC is the*
 497 *soil water storage capacity.*

498

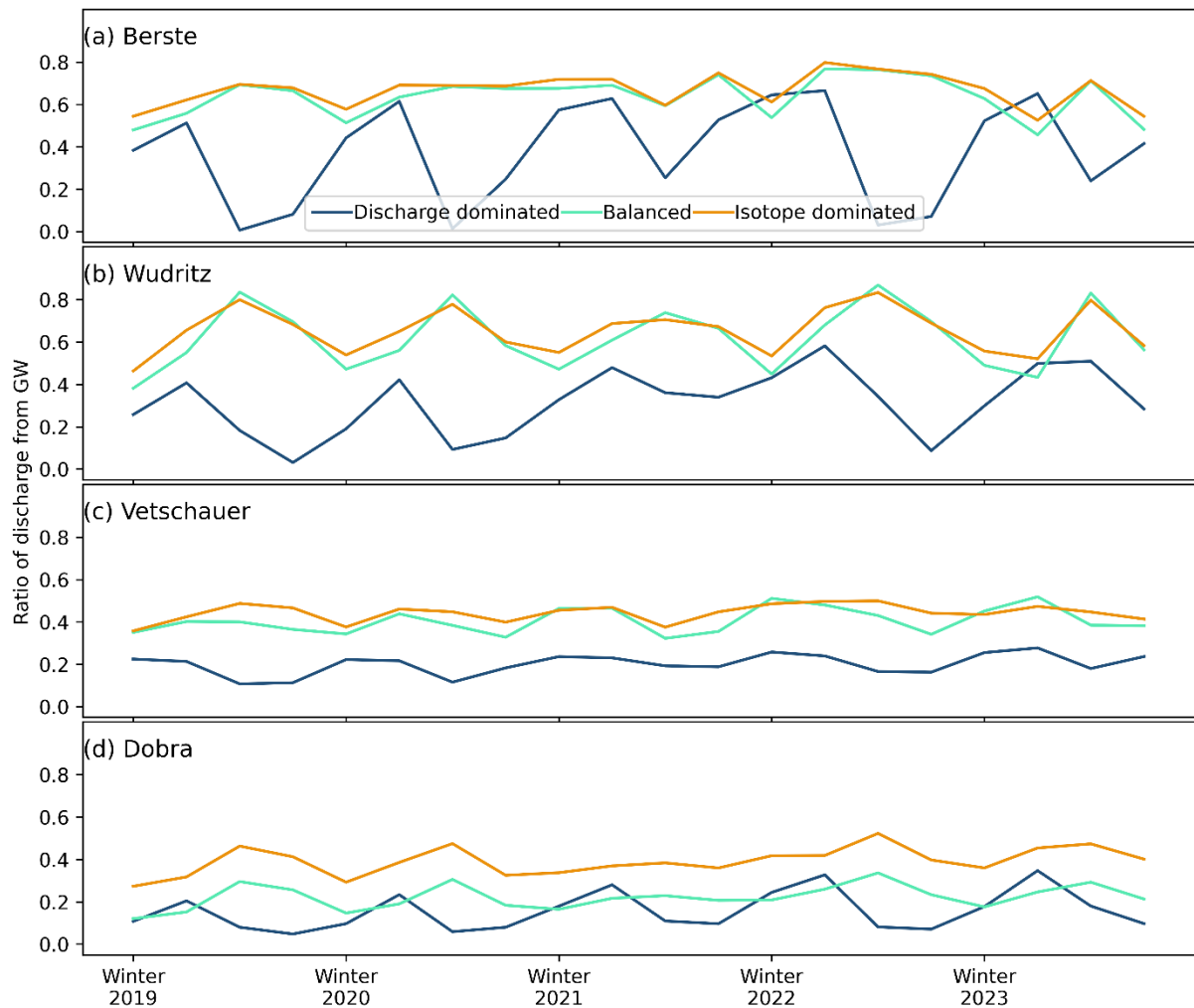
499 3.2.2 Impact of calibration on contributing runoff generation processes

500 Runoff generation from soil storage was the most sensitive hydrological processes in the
 501 simulations in all calibration schemes (no matter whether isotope measures were considered),
 502 while groundwater (GW) contributions were highlighted by isotopes in Berste and Vetschauer

503 ~~(Table 4). According to the~~Figure 5). Contrasting GW contributions to discharge were shown
504 ~~in different solution types of the isotope-aided calibrations (Figure 6). In the discharge-~~
505 ~~dominated solutions on the Pareto front, runoff was mostly generated from the soil and~~
506 ~~groundwater storages, while overland flow was limited in the pasture in the winter or spring of~~
507 ~~the wet year of 2023 in two of the catchments (Figure 5). For the parameter sets that produced~~
508 ~~the best streamflow simulationsschemes 2-5,~~ runoff was mainly sourced from the shallower
509 soil stores ~~in all three major land uses,(soil storage in the STARR),~~ while this contribution
510 ~~gradually decreased in simulations for the opposite end of the Pareto frontthe isotope-~~
511 ~~dominated solutions~~ with groundwater sources being more important ~~for simulations with~~
512 ~~better isotope performance (Figure 5).(Figure 6). Summer peaks of groundwater contribution~~
513 ~~shown in the isotope-dominated and balanced solutions aligned better with the known~~
514 ~~hydrological regime of the local region (e.g. Ying et al., 2024), compared to discharge-~~
515 ~~dominated solutions (Figure 6). Among the four catchments, higher groundwater contributions~~
516 ~~were shown in Berste and Wudritz, reaching 60% in isotope-dominated or balanced solutions~~
517 ~~(Figure 6).~~

518

519



520

521 *Figure 5. Total 6. The mean ratio of seasonal runoff from contrasting sources for three land*
 522 *uses for groundwater storage at each catchment during 2019 and 2023 (winter, spring, summer,*
 523 *fall of 2019 and 2023 each year along the X-axis). The results were calculated from bottom*
 524 *up, and “W” the discharge dominated, balanced and isotope dominated solutions in the Y label*
 525 *means winter) in the first Pareto front of (a) Berste (scheme 2); (b) Wudritz (scheme 3); (c)*
 526 *Vetschauer (schemes 2-5).*

527

528 *4); (d) Dobra (scheme 5). “QGsim” and “Qsm” represent runoff from groundwater and soil*
 529 *water, respectively, while “QSSim” is instantaneous overland flow. Each pixel in the plot is*
 530 *the total seasonal amount of runoff. The X axis from left to right represents results from BSI to*
 531 *BSS.*

532
533
534
535
536
537
538
539
540
541
542
543
544
545
546
547
548
549
550
551
552
553

Runoff generation from soil and groundwater storages showed seasonality with higher streamflow in winter. This pattern was further intensified during the wet year of 2023 (Figure 5). Runoff from soil in parameter sets with better simulated streamflow presented lower influence in croplands of all four catchments. Runoff from groundwater in simulations with better isotope performance was more evident in croplands than the other two land uses, except for the Vetschauer catchment (Figure 5). Subsurface water flowing through capillary flux (from groundwater storage to soil) and soil seepage (soil to groundwater) was consistent along the Pareto front of Wudritz and Dobra, with high contribution of both fluxes in croplands (Figure S3). The stronger influence of subsurface processes in Berste and Vetschauer was only reproduced in simulations with better isotope performance (Figure S3).

Table 4. Performance metric values (KGE) of simulated spatially averaged ET in the scheme 1 and balanced solutions of schemes 2-5 based on remote sensing products at the studied catchments.

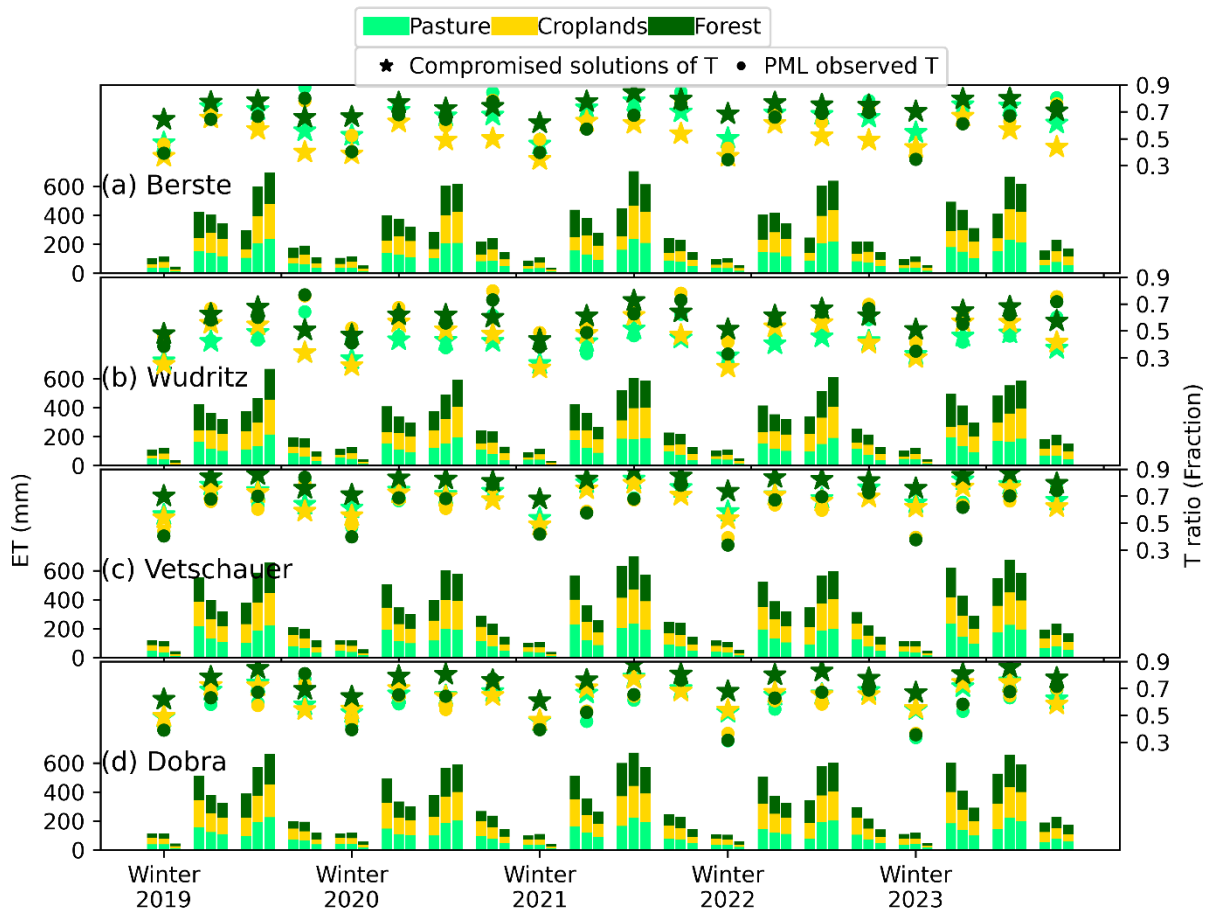
<u>Locations</u>	<u>Scheme1</u>		<u>Schemes 2-5</u>	
	<u>MODIS</u>	<u>PML</u>	<u>MODIS</u>	<u>PML</u>
<u>Berste</u>	<u>0.59</u>	<u>0.46</u>	<u>0.45</u>	<u>0.36</u>
<u>Wudritz</u>	<u>0.59</u>	<u>0.45</u>	<u>0.78</u>	<u>0.59</u>
<u>Vetschauer</u>	<u>0.56</u>	<u>0.42</u>	<u>0.77</u>	<u>0.62</u>
<u>Dobra</u>	<u>0.56</u>	<u>0.44</u>	<u>0.77</u>	<u>0.64</u>

3.2.3 Impact of calibration on ET estimates and ET partitioning

The ~~sensitivity of~~ parameters controlling the ~~movement~~return flux of water to the atmosphere (ET) ~~was important, although they had contrasting order in each~~ were sensitive to the use of both discharge and isotopes in calibration scheme. Except for the underestimated ET in parameter sets with better(Figure 5). Further, spatially averaged ET in the balanced solutions of all schemes aligned well with both remote sensing products (MODIS and PML), supporting the robustness of the calibrations, although the trade-offs between discharge and isotopes at

554 ~~Berste resulted in a degraded performance in the Scheme 2 (Table 4). All solution types in the~~
555 ~~isotope-aided calibrations generally showed only slight differences, except for croplands in~~
556 ~~Berste and Wudritz, where the discharge-dominated solutions simulated isotopes in Berste,~~
557 ~~parameter sets along the Pareto front had consistent annual higher ET volume in each~~
558 ~~catchment (from 400 to 500 mm/year in dry to wet years), and mostly aligned with both satellite~~
559 ~~estimates. (Figure S6). ET showed strong seasonality with peaks in spring and summer in model~~
560 ~~simulations all solution types (Figure 67; Figure S4S6). This aligned was consistent with the~~
561 ~~satellite ET observations. Simulations at both ends of the Pareto front However, balanced~~
562 ~~solutions showed higher springtime ET yet lower modelled ET in summer across all catchments~~
563 ~~compared to the remote sensed products, except for BSI in Berste. due to limited soil moisture.~~
564 ~~These differences decreased during wet summers (e.g., 2021 and 2023) (Figure 6; Figure S4).~~
565 ~~BSI (except for Berste) in schemes 2-5 had lower spring ET and higher summer ET compared~~
566 ~~to BSS. This seasonal shift in BSI aligned better with temporal patterns of remote sensed ET~~
567 ~~(Figure 6).~~

568



569

570 *Figure 67. Seasonal total ET and transpiration ratio (T/ET) from simulations the balanced*
 571 *solutions at (a) Berste in scheme 2; (b) Wudritz in scheme 3; (c) Vetschauer in scheme 4; (d)*
 572 *Dobra in scheme 5, and RS products. Bars and lines scatters indicate ET and T ratios,*
 573 *respectively. Each season contains four three bars, ordered from left to right as follows:*
 574 *simulation with best simulated isotope and best streamflow balanced solutions, MODIS and*
 575 *PML ET products. ET values from each land use were scaled according to their area*
 576 *proportion, and the stacked bar value approximately represents the total seasonal ET of the*
 577 *sub-catchment.*

578

579 Simulations ET in scheme 1 and BSS (the discharge-dominated solutions of schemes 2-5)

580 exhibited higher consistency with presented a relatively uniform spatial patterns of MODIS

581 ET compared to BSI (schemes 2-5). Additionally, elevated ET was consistently captured along

582 ~~the channel reach in Berste, distribution, while the upper catchment in Wudritz, and across the~~
583 ~~whole catchment of Vetschauer and Dobra (Figure 7), although the simulated balanced or~~
584 ~~isotope-dominated solutions retained more pronounced spatial variability ~~in ET remained less~~~~
585 ~~pronounced than, aligned with the MODIS estimates. (Figure 8; Figure S7). However, no~~
586 ~~solutions successfully captured the distributions of ET in the MODIS or PML. In addition, high~~
587 ~~ET in the PML product was more consistent with croplands distribution, which indicated the~~
588 ~~potential influence of irrigation in croplands that has and were not been conceptualized shown~~
589 ~~in the current model structure MODIS, reflecting the uncertainty of accuracy of spatial~~
590 ~~distributions in these remote sensing products. (Figure 78).~~

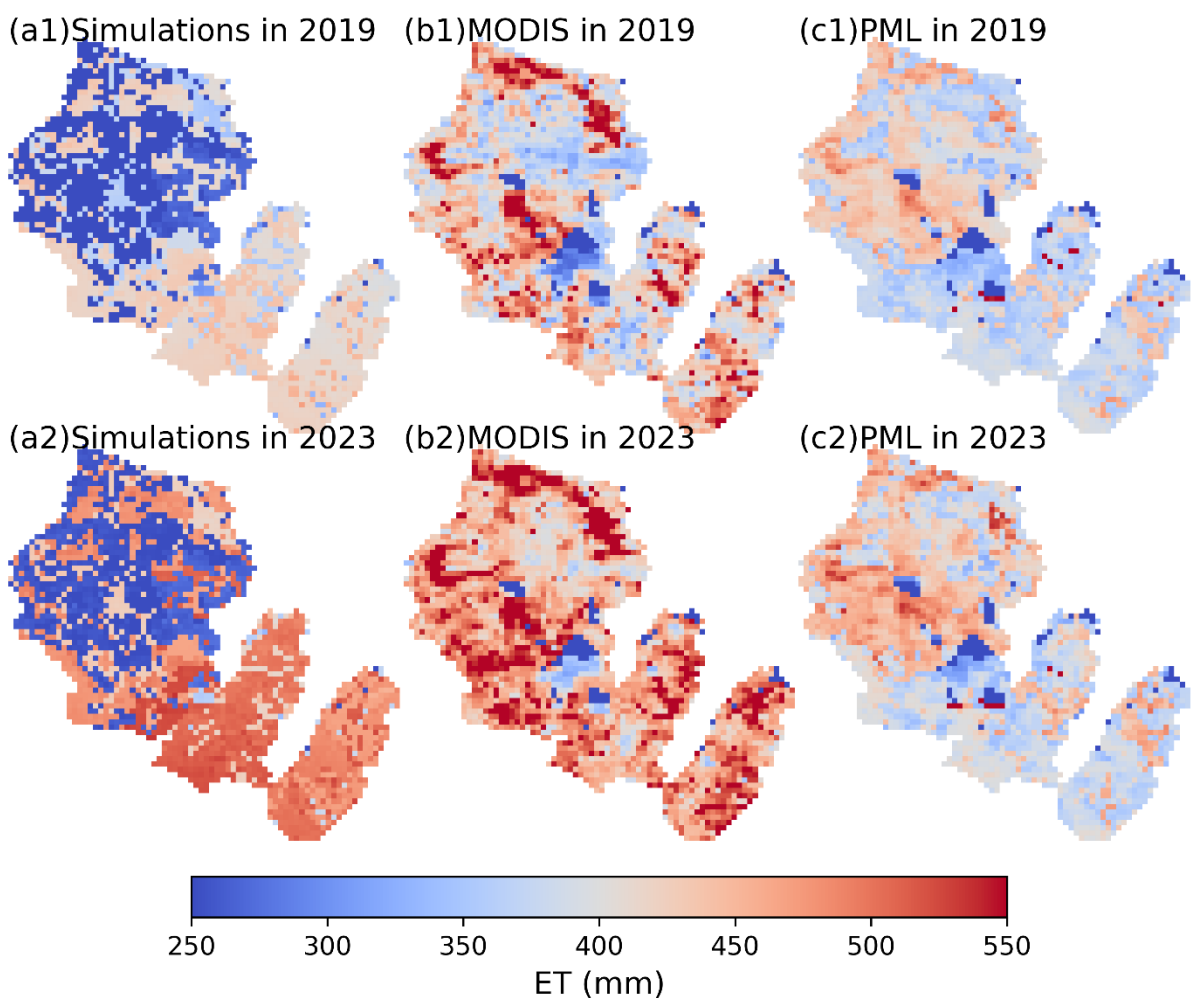
591

592 ~~In terms of ET partitioning (into E and T), soil water storage capacity) became more sensitive~~
593 ~~for simulations constrained by isotopes as the corresponding parameters (K) ranked higher~~
594 ~~compared to Scheme 1 or discharge-only based simulations dominated solutions in Schemes~~
595 ~~2-5. This is consistent with the importance of fractionation in the variation of isotopes (Table~~
596 ~~4 Figure 5). In all catchments, the transpiration ratio from each land use had similar temporal~~
597 ~~dynamics (summer peaks and winter troughs), and was higher in forest than in the other two~~
598 ~~land uses (Figure 6; Figure S4). In Vetschauer, most simulations of transpiration ratios in the~~
599 ~~Pareto front in all three land uses aligned with the PML estimates, with 50-70% and 30-40%~~
600 ~~(dependent on land use; with forest being higher) in summer and winter shown in compromised~~
601 ~~solutions, respectively, although with slightly lower values in BSI. The consistent and high~~
602 ~~transpiration along the Pareto front was shown in Berste, and only some of the better simulated~~
603 ~~isotope simulations in the Pareto front highly underestimated transpiration (Figure 6, Figure~~
604 ~~S4). In contrast, simulations (schemes 2 and 5) in Wudritz and Dobra showed notably lower~~
605 ~~transpiration ratios, and only a small part of simulations in the Pareto front reached RS levels~~
606 ~~(Figure S47; Figure S8). Berste, Dobra and Vetschauer yielded higher transpiration ratios, with~~

607 70-80% and 40-60% in summer and winter, respectively, compared to Wudritz. Further,
 608 Wudritz was ~10% lower (compared to other catchments) in transpiration ratio, aligned well
 609 with the PML estimates. In addition, Berste and Wudritz showed contrasting performances
 610 among different type of solutions (discharge-dominated, balanced or isotope-dominated
 611 solutions), with discharge-dominated solutions showing higher ratios (Figure S8).

612

613



614

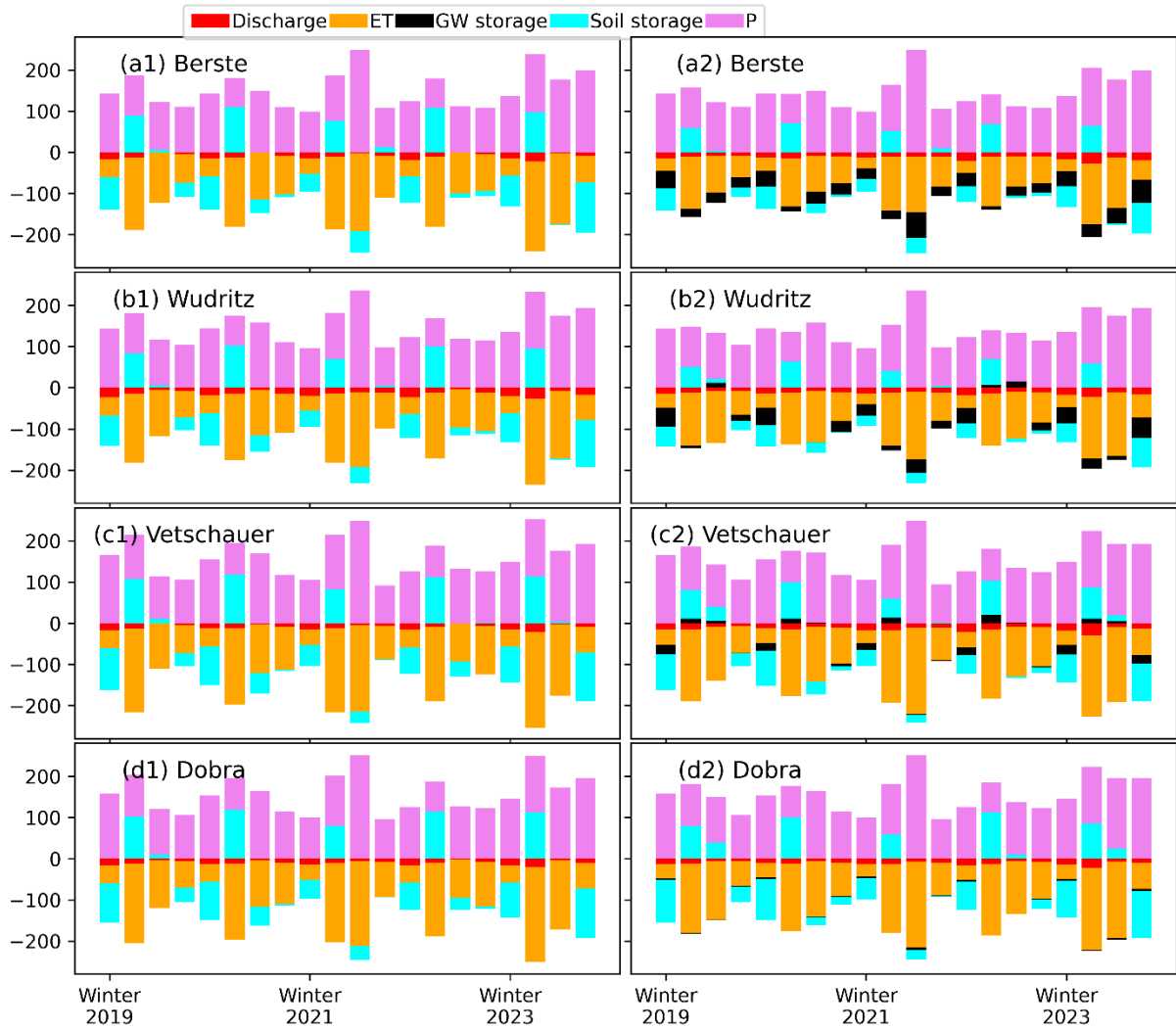
615 *Figure 78. Spatial distribution of ET in the four catchments. (a) Scheme 1; (b) BSS Balanced*
 616 *solutions in schemes 2-5; (c) BSI in schemes 2-5; (d) b) MODIS ET; (e) PML ET. Suffix “1”*
 617 *and “2” means in titles of each subplot mean dry year of 2019 and wet year of 2023,*
 618 *respectively.*

619

620 3.3 Quantification of ~~the~~ water balance components

621 The partitioning into different water balance components was relatively consistent across all
622 catchments, irrespective of the calibration schemes (Figure 89). ET was the dominant output
623 flux, especially during the spring and summer period (> 90%). Simulations showed that soil
624 storage played the major role in supplying water for ET in spring and early summer and was
625 subsequently replenished during autumn and winter. Discharge accounted for a minor
626 proportion of the water balance (~5%). Variations of groundwater storage in each season were
627 small (<1% of the total water balance) in simulations calibrated on discharge alone, while it
628 increased to ~5 - 30% (catchment dependent) when isotopes were included in calibrations
629 (Figure 8). ~~With isotopes in calibrations, simulated groundwater storage declined during spring
630 and summer and was replenished in winter and fall, with the variation being the most
631 substantial in Vetschauer-9). A clear seasonal pattern of groundwater dynamics was shown in
632 Vetschauer, with declining storage during the spring and summer and replenishment in winter
633 and fall. In contrast, the groundwater storage kept increasing in each season at Berste, while
634 this storage only occasionally decreased in summer at Wudritz and Dobra (Figure 9). The
635 annual increased in subsurface storage aligned with the gradually recovery of the groundwater
636 level in this region following the 2018-2019 drought (Figure S9).~~

637



638

639 *Figure 89. Seasonal water balances in the four catchments at (a) Berste; (b) Wudritz; (c)*
 640 *Vetschauer; (d) Dobra. Suffix “1” and “2” means averaged values of all simulations, based*
 641 *on the balanced solutions in the Pareto front of calibration scheme 1 (first panel (a1, b1, c1,*
 642 *d1)) and a compromised solution in schemes 2-5, respectively (second panel (a2, b2, c2 d2)).*

643 *Positive bars represent water sources, while negative bars are water losses. “Channel storage”*
 644 *and “Interception storage” were too small compared to other components to show in the figure.*

645 **4 Discussion**

646 **4.1 Model success for streamflow and isotope dynamics**

647 The key novelty of this study lies in evaluating the use of multi-year, seasonally sampled
648 isotopes for calibrating a TAM to ET-dominated and heavily managed catchments. Previous
649 catchment-scale TAM applications have generally been in smaller experimental catchments
650 with limited human influences (Nan and Tian, 2024). Whilst such work has demonstrated the
651 value of isotopes in constraining hydrological models, the present study has shown similar
652 potential benefits in heavily managed regions. Furthermore, the trade-offs between using
653 discharge and/or isotopes in model calibration showed that isotopic information can still
654 provide valuable preliminary process insights. The observed inter-catchment differences in
655 isotope variations were influenced by the interaction of dominant runoff sources, associated
656 mixing processes with water storages and the effects of evaporative fractionation; capturing
657 these in simulations were, in turn, linked to modelled discharge performance. The response of
658 runoff to rainfall, seasonal flow variations and baseflow contribution derived from discharge-
659 calibrated models showed inconsistency with isotope-inferred processes. Given that
660 contrasting trade-offs were identified among catchments within the same region, these
661 discrepancies are likely to in part reflect undocumented influences of human management and
662 provide a potential pathway to model improvement.

663

664 **4.1 Benefits of incorporating isotopes into model calibration**

665 ~~Streamflow usually serves as a key indicator of water resource availability and is~~ most widely
666 ~~used in hydrological model calibration due to its broad accessibility. Previous work using~~
667 ~~isotopes and other tracers has shown that calibration on streamflow alone can lead to~~
668 ~~misleading conceptualization of hydrological processes (Ala-Aho et al., 2017; ready~~

669 availability. Here, similar to many previous ~~van Huijgevoort et al., 2016; McDonnell and Beven~~
670 ~~2014). However, similar to most~~ studies based in environments where blue water fluxes (i.e.
671 ~~streamflow and groundwater recharge) are greater than green water fluxes (i.e. ET fluxes that~~
672 ~~sustain vegetation growth), here,~~ streamflow dynamics and overall runoff volumes were ~~also~~
673 effectively captured by discharge-only based calibrations ~~in and despite the~~ ET-dominated
674 ~~region dominance.~~ However, slight overestimations of flow occurred during winter peaks ~~and,~~
675 with underestimations during summer low-flow ~~periods~~ flows. In addition, ~~modelled~~
676 ~~annual~~ simulated spatially averaged ET ~~estimates~~ (weekly flux) aligned closely with RS ET
677 products (e.g., MODIS or PML), with ~~ET amounts ~400–500 mm/year from dry (e.g., 2018)~~
678 ~~to wet (e.g., 2023) years and deviation of around ± 50 mm/year. KGE > 0.5.~~ Although
679 groundwater recharge was ~~sometimes underestimated (especially in Berste), rough~~ implausibly
680 low, approximate partitioning of precipitation into green and blue water fluxes was accurately
681 constrained by streamflow ~~in the~~ calibrations. Similarly, in some other ~~literatures~~ literature,
682 multi-criteria calibrations incorporating both streamflow and RS ET demonstrated marginal
683 improvements in annual ET or streamflow ~~estimates~~ simulations, compared to discharge-only
684 based calibrations, albeit with reduced parameter equifinality (Oliveira et al., 2021; Shah et al.,
685 2021). Though in other cases they have not been beneficial. (Ala-aho et al., 2017b).

686

687 However, Previous work using tracers has shown that based on calibration on streamflow alone
688 can result in the wrong conceptualization of hydrological processes (Ala-Aho et al., 2017a; van
689 Huijgevoort et al., 2016; McDonnell and Beven 2014). ~~However, discharge~~ Discharge-only
690 based calibrations normally exhibit significant uncertainty in representing internal hydrological
691 processes, owing to high degrees of model freedom and non-identifiable parameters (Herrera
692 et al., 2022). This was evidenced by ~~the large uncertainty bands in the~~ poorly simulated
693 ~~variables (for both streamflow and isotopes)~~ under scheme 1. Moreover, catchment discharge,

694 as an output integrating upstream hydrological processes, provides only limited insight into
695 spatially distributed partitioning of water volumes and flow paths (Fatichi et al., 2016). This
696 limitation becomes more pronounced as models incorporate more complex spatial
697 disaggregation and physics-based process representations (Sun et al., 2017). A multi-gauge
698 regional streamflow calibration, as used in Scheme 1, normally improves the spatial
699 representativeness of simulations and provides a greater constraint on relationships between
700 catchment characteristics and streamflow dynamics (Liu et al., 2020). However, internal
701 mixing and runoff generation processes (evidenced by isotope dynamics) under scheme 1
702 ~~(which was a multi-gauge streamflow calibration)~~ did not show much difference to the single-
703 gauge calibrations (i.e., ~~parameter set with best simulated streamflow discharge-dominated~~
704 solutions in schemes 2-5). Improvements on simulations of subsurface processes were also not
705 clear in other literature (Wanders et al., 2014). Furthermore, sensitivity analysis revealed that
706 discharge was more sensitive to soil drainage process in all three major land uses (i.e., forest,
707 croplands, pasture) of the four studied catchments, and parameters controlling other
708 hydrological processes were less identifiable.

709

710 Incorporating stable water isotopes ~~into~~improved modelling ~~improves our understanding of~~
711 ecohydrological ~~processes~~partitioning and storage dynamics. ~~in our study~~. Multi-criteria
712 calibration using both streamflow and ~~isotope isotopes~~ enables a wider exploration of ~~a~~
713 ~~broader~~the parameter space to satisfy multiple calibration objectives (Holmes et al., 2020).
714 Subsurface processes in the deeper layer (e.g., ~~seepage and capillary flux~~discharge from
715 groundwater in the present ~~model~~modelling) are inherently challenging to constrain ~~in~~
716 ~~modelling through only using~~ near-surface observations (e.g., ET, soil moisture), and these
717 processes are usually poorly understood (Beven, 2006). Stable water isotopes are powerful in
718 this regard as they integrate the cumulative effects of water flow paths and mixing across all

719 hydrological storages (Godsey et al., 2010); Tafvizi et al., 2024). Our TAM revealed that
720 discharge-only based calibration or ~~parameter sets with better simulated streamflow discharge-~~
721 ~~dominated solutions~~ in isotope-aided calibrations ~~does not accurately failed to~~ capture such
722 mixing processes, as their simulated isotopes ~~are different~~deviated far from observations.
723 ~~Model simulations~~Modelling results that reconciled simulated and observed isotopes likely
724 better represented ~~better~~ mixing between soil water and groundwater storage. ~~Increased~~This
725 generally increased runoff generation from groundwater, characterized by more depleted
726 isotopes, and modulated ~~modelled~~simulated outflow signatures, flattening the seasonal isotopic
727 variability, and thus, ~~increasing~~giving more plausible process representation. This aligns with
728 previous findings where dominant subsurface flows produce subtle isotopic variations
729 (Iorgulescu et al., 2007; Oerter and Bowen, 2019) and where contrasting isotope signatures
730 across water stores are key to disentangling water mixing processes (Kirchner, 2003).

731

732 The fractionation of stable water isotopes is governed by evaporation, and measured isotopes
733 at the ~~catchment~~ outlet reflected the aggregated influence of evaporation ~~rates~~ across the whole
734 catchment. Parameters controlling ET processes (e.g., FC and LP) exhibited ~~greater~~similar
735 sensitivity ~~when using to~~ isotopes ~~as a calibration target and discharge~~, supporting ~~its~~the value
736 of isotopes as a constraint on ET dynamics in simulations. ~~Despite this~~This is similar to the
737 incorporation of remote sensed ET in calibrations found in other literatures (Oliveira et al.,
738 2021). In addition, total (~~bulk~~) seasonal ET volumes across the catchments showed minimal
739 variations ~~along~~among different solution types in the Pareto front, implying that streamflow
740 and isotopes similarly constrain bulk ET estimates. The use of ~~temporally quite~~relatively coarse
741 isotopic datasets ~~—necessary at such large spatial scale—~~ and inter-annually averaged rainfall
742 isotope inputs in this study likely introduced some uncertainty in ET process constraints, and
743 higher-resolution data ~~can~~would better capture temporal variability in fractionation intensity

744 (Sprenger et al., 2017). ~~This is~~ Nevertheless, the results are reasonable and consistent with
745 broader findings in the literature: while isotopic tracers are widely recognized for improving
746 estimates of E/T partitioning (Gibson and Edwards, 2002), their utility in refining total ET
747 quantification prior to discharge remains less clearly demonstrated, particularly at larger spatial
748 scales.

749

750 **4.2 ~~Water~~ Isotopic insights into water flux partitioning in managed catchments and** 751 **influences of management measures**

752 ~~Compared to simulations in the Berste, the ecohydrological partitioning was more reliably~~
753 ~~represented in the Wudritz, Vetschauer and Dobra, as NSE or KGE of both streamflow and~~
754 ~~isotopes reached > 0.4 in the compromised solutions (middle part of Pareto optimal solutions).~~

755 ~~In these~~

756 In the studied catchments, runoff was predominantly generated from groundwater and soil
757 storage, reflecting a subsurface-process dominated flow regime. This pattern aligns with
758 observations across much of the Spree catchment, where subsurface-driven runoff mechanisms
759 are widespread (Chen et al., 2023). Runoff in the upper Spree catchment is predominantly
760 groundwater-driven (Kröcher et al., 2025), a pattern consistent with the ~~Vetschauer catchment,~~
761 ~~and likely shared by the Berste, as evidenced by depleted isotopic signatures. In contrast, the~~
762 ~~Wudritz and Dobra catchments showed rather lower proportions of groundwater contributions.~~
763 ~~This aligns with historically depressed groundwater levels caused by pumping during regional~~
764 ~~de-watering from mining activities (Arndt and Heiland 2024).~~ simulated performance in the
765 studied region after incorporation of isotopes. In addition, the influence of groundwater in the
766 studied four catchments may potentially increase, as the opencast mines have been closed for
767 30 years and it is unclear to whether groundwater levels have fully stabilized and how they

768 affect each of the study catchments (Kröcher et al., 2025). The increased temperature and shift
769 of precipitation from summer to winter due to climate change also possibly leads to increased
770 ET during winter and spring reducing discharge and groundwater recharge accordingly. This
771 could result in contrasting water distributions in each season, and intensifying negative climatic
772 water balance in the local environment (Pohle et al., 2012).

773

774 ~~In Wudritz~~ The transpiration ratios in the studied region were roughly 65% in the PML
775 estimates, which is similar to other studies in the Spree catchment (Landgraf et al., 2022).
776 However, simulated transpiration ratios at Berste, Vetschauer and Dobra, isotope simulations
777 optimized for streamflow accuracy produced were ~10% higher than the PML estimates,
778 consistent with the limited fractionation shown in the streamwater isotopes. The temporally
779 coarse sampling potentially underestimated the seasonally aggregated fractionation, but the
780 general seasonal variations were captured in the data. In addition, uncertainties in this remote
781 sensing product cannot be discounted. In contrast at Wudritz, the simulated ratios were more
782 isotopically depleted signatures compared to the measured consistent with the PML values. To
783 reconcile this discrepancy, an assumption of lower proportions of transpiration in
784 evapotranspiration (ET) was needed. The mismatch in transpiration ratios ~~between simulations~~
785 ~~and the PML product~~ may partially stem have resulted by underestimated evaporation from
786 calibration with seasonally sampled isotopes, though this may be counterbalanced by
787 unaccounted surface water evaporation, from lakes in the former mining area. While
788 evaporation from small open water bodies ~~(e.g., ponds, channels)~~ has negligible impacts on
789 overall the catchment water balance, it ~~likely plays a critical~~ can play an important role in
790 isotopic enrichment (Birkel et al., 2011). For instance: in the ~~Dobra (3.0% surface water area)~~
791 ~~and~~ Wudritz (7.7% surface water area), isotopic concentrations in simulations were likely
792 underestimated due to unmodeled surface water evaporation. The non-linear relationship

793 between evaporation rate and isotopic enrichment, as described by the Craig-Gordon model
794 (Craig and Gordon, 1965), explains this dynamic: early-stage evaporation induces stronger
795 isotopic enrichment, approaching a threshold under constant environmental conditions (e.g.,
796 humidity, temperature). Thus, even relatively minor surface water evaporation can bias isotopic
797 signatures which then impacts ET partitioning simulations.

798

799 ~~In contrast, at Vetschauer (0.7% surface water area), the unaccounted surface water evaporation~~
800 ~~had minor effects on the modelling due to the minimal surface water area with simulations~~
801 ~~being more comparable to the PML estimates. The ability of stable water isotopes in~~
802 ~~constraining ET partitioning was also shown in the consistency between simulations and the~~
803 ~~PML estimates, which is similar to other applications (Birkel and Soulsby, 2015).~~ Further, the
804 small weight of isotopes in a scalar function combining multiple objectives meant that it was
805 possible to help disentangle ET processes (Wu et al., 2023). This was also illustrated by the
806 minor adaptations ~~in the Pareto front from better streamflow simulations to better isotope~~
807 ~~simulations. The transpiration ratios in the simulations~~ along the Pareto front ~~with better~~
808 ~~simulated isotopes~~ at Vetschauer ~~also aligned with the other sub-catchments of the Middle~~
809 ~~Spree (Landgraf et al., 2023) and Dobra.~~ The normally contrasting transpiration ratios
810 amongbetween different land uses (Schlesinger and Jasechko, 2014) were consistent with our
811 simulations, and ~~contrasting LAI~~ divergent LAIs in each land use explains these differences
812 (Cao et al., 2022), although the PML estimation presented similar transpiration ratios among
813 each land use. However, the transpiration ratios could be ~~overestimated~~ underestimated in
814 specific land uses due to unparameterized irrigation effects (Paul-Limoges et al., 2022), and
815 the local water use efficiency ~~should be further evaluated. The strong conflicts between using~~
816 ~~streamflow or isotopes as calibration constraints resulted in incorrect representation of~~
817 ~~transpiration ratios in Berste (0.3% surface water) along the Pareto front near the BSI. However,~~

818 ~~simulations near the BSS still indicated a first approximation of transpiration, considering the~~
819 ~~effectiveness of isotopes in differentiating ET partitioning, needs to be further evaluated to~~
820 ~~improve future modelling.~~

821

822 Despite uncertainties introduced by ~~multiple anthropogenic factors and influences~~relatively
823 ~~coarse sampling~~, isotopes were still valuable in ~~ET~~water partitioning (i.e., ET and runoff) in
824 such heavily managed ~~catchment. Since the Middle Spree is~~catchments, which has been shown
825 ~~to be an~~ advantage compared to other potential calibration targets (e.g., ~~ET-dominated region~~
826 ~~and experiencing water scarcity due to replenishment of historical groundwater withdrawn,~~
827 ~~evaluation of local water use efficiency in the croplands is of great value for future water~~
828 ~~management, soil moisture; Wu et al., 2023). The preliminary assessment of ET partitioning~~
829 through isotope-aided modelling provides ~~evidence for assessing the water-use efficiency of~~
830 ~~different land uses, especially croplands. Isotope data at finer temporal resolution would likely~~
831 ~~help better constrain ET partitioning in such heavily modified catchments, as they do in less~~
832 ~~disturbed environments (Tunaley et al., 2017; Soulsby et al., 2015). In addition, precipitation~~
833 ~~isotopes were from a global data product (Bowen et al., 2005). The use of interannually~~
834 ~~averaged monthly values likely failed to capture short-term climate variability or anthropogenic~~
835 ~~influences (e.g., strong evidence in this aspect, although its~~fossil fuel-derived vapor), and may
836 ~~introduce uncertainties in water source apportionment (Xia et al., 2024; Yang and Yoshimura,~~
837 ~~2024), though given the groundwater dominance and older (>5 years) ages of runoff (Smith et~~
838 ~~al., 2021), the effects are likely to be small. Again, high resolution local data would be~~
839 ~~advantageous to improve such estimates.~~

840

841

842 **4.3 Insights from contrasting discharge-isotope trade-offs ~~with streamflow occasionally~~**
843 ~~occurred due to unaccounted human impacts.~~ **among the four catchments**

844
845 **4.4 ~~Reasons for trade-offs between ecohydrological fluxes and future research directions~~**

846 Trade-offs in the calibrations between streamflow and isotopes are a well-known feature of
847 TAM (Holmes et al., 2020), though their severity varies across applications. The extent of these
848 compromises depends on the model's structural flexibility to assimilate additional constraints
849 ~~(Holmes et al., common feature of TAM (Holmes et al., 2020), though their severity varies~~
850 ~~across applications. The extent of these compromises depends on the model's structural~~
851 ~~flexibility to assimilate additional constraints (Holmes et al., 2020).)~~ **and the weightings given**
852 **(Wu et al., 2025).** Whilst some applications based on spatially-distributed models presented
853 ~~slight~~ **relatively minor** conflicts in the information content of different calibration targets
854 (Kuppel et al., 2018), significant ~~degradations~~ **degradation** in streamflow ~~is~~ **performance has**
855 **been** found in ~~a~~ **lumped models** after incorporating isotopes in calibration (Fenicia et al., 2008).
856 ~~model after incorporating isotopes in calibration (Fenicia et al., 2008).~~ In our study, the lack of
857 explicit ~~information on~~ **representation of some** anthropogenic drivers (e.g., water ~~withdrawals,~~
858 ~~irrigations~~ **abstraction, irrigation** etc.) **in the model** emerged as a **key** **likely** contributor to trade-
859 offs. Without ~~parameterizing~~ **explicit parameterization for** these factors, the model
860 ~~compensated by adjusting~~ **often failed to fully capture** flow ~~velocities, which failed to replicate~~
861 ~~observed streamflow celerity during rainfall events. The~~ **dynamics in the catchments.**

862
863 ~~There was evidence for such~~ systematic biases ~~were evidenced: parameter sets with better~~
864 ~~simulated streamflow.~~ **For example, discharge-dominated solutions** in isotope-aided
865 calibrations produced a soil water-driven runoff regime ~~and underestimated baseflow, which~~
866 ~~were exacerbated by spring or~~ **that generally underestimated baseflow. The STARR model**

867 derived a fast draining process in the shallow subsurface layer (soil storage in the STARR) to
868 simulate flattened isotope variations. Water in the shallow subsurface flows to the outlet
869 through direct discharge (faster draining lead to lower evaporation and lower fractionation) and
870 to the groundwater through seepage (high groundwater storage flattening isotope variations).
871 In terms of discharge, high groundwater storage would typically result in flattened seasonal
872 variations and elevated baseflows, whereas rapid draining of soil storage to discharge resulted
873 in quick runoff response to rainfall, as illustrated by the isotope-dominated solutions (Figure
874 S4). However, in the studied region, only the Vetschauer catchment showed both a rapid
875 response to rainfall and high baseflow, and therefore showed relatively minor trade-offs
876 between isotopes and discharge in the modelling. In contrast at the Berste catchment, discharge
877 exhibited low base flow and pronounced seasonal variations but lacked a rapid response to
878 rainfall events, which was inconsistent with the hydrological processes inferred by isotope
879 observations. As all four catchments are located within the same region, with broadly similar
880 soil cover, it might be expected that the soil hydrological response would be similar among the
881 four catchments. However, the Berste, with the largest area, had the lowest base flows and
882 slower responses to rainfall events compared. Considering the Berste catchment has the most
883 extensive cropland coverage and high (but unknown) irrigation withdrawals, these trade-offs
884 could be potentially explained by management measures. Moreover, the higher groundwater
885 contribution at Berste and Wudritz, compared to Vetschauer and Dobra, might be explained
886 irrigation water withdrawals. Extraction of groundwater to the surface could dampen isotope
887 variations in stream water, although much of the water volumes are expected to evaporate
888 during summer water withdrawals altering natural flow regimes. Measured isotopic damping
889 (flattened variations) implied slower flow velocities and greater groundwater contributions, yet
890 the model was unable to capture these processes from streamflow dynamics alone. The
891 strongest trade-offs occurred in the Berste catchment, where extensive croplands and likely

892 ~~high irrigation withdrawals amplified mismatches~~period. Therefore, the un-represented water
893 ~~extraction process likely introduces more conflicts~~ between simulated and observed
894 ~~hydrological behavior~~discharge and isotope observations.

895

896 These trade-offs ~~could~~would likely be ~~partially~~mitigated by ~~integrating~~more process-based
897 conceptualizations, ~~of anthropogenic impacts (e.g. irrigation)~~, though ~~this often requires more~~
898 ~~complex parameterizations~~. While such enhancements improve a model's ability to
899 ~~simultaneously adapt flow velocity and celerity~~, they also ~~introduce~~at the expense of greater
900 ~~simulation~~parameterization and higher uncertainty (Herrera et al., 2022). ~~Simple explicit~~
901 ~~modeling of water extraction for irrigation (e.g., channel to cropland transfers)~~ could alleviate
902 ~~trade-offs observed in this study~~. However, ~~sparse records of withdrawal volumes and~~
903 ~~irrigation patterns, as well as political sensitivities in data sharing may limit practical modelling~~.

904 The STARR model's simplified routing structure, where runoff from contrasting sources
905 follows identical pathways to the outlet, diverges from more physics-based frameworks that
906 better spatially differentiate the timing of contributions of overland flow, unsaturated zone flow,
907 and groundwater flow. ~~While this~~This conceptual routing ~~captured~~can capture flow ~~celerity by~~
908 ~~adjusting discharge coefficients (i.e., kS, kG)~~, it systematically overestimateddynamics in the
909 ~~stream, but likely mis-represent~~ flow ~~velocity~~partitioning and creating conflicts in multi-
910 criteria calibrations (McDonnell and Beven 2014). ~~An additional point is that STARR didn't~~
911 ~~include any consideration of channel leakage and parameterization of the hyporheic flow could~~
912 ~~potentially and partly explain the flattened isotope variation and over-estimated baseflow~~
913 ~~simulations. This is a particular problem in former mining areas where recovery after historic~~
914 ~~groundwater is incomplete or has altered local groundwater surface water interactions~~
915 ~~increasing the possibility of streams having "losing" reaches with vertical leakage into~~
916 ~~groundwater (Pohle et al., 2025)~~.

917

918 Further, STARR calculates ET solely based on water availability and partitions PET into PE
919 and PT using a simplified single calibrated parameter. In contrast, more physically-based
920 models, such as EcH2O-iso (Kuppell et al., 2018), explicitly simulate runoff generation
921 processes and compute ET through coupled energy and water balance equations, and thus likely
922 better integrate isotopic information. While such enhancements improve a model's ability to
923 simultaneously reconcile flow velocity and celerity, they also introduce greater parameter
924 uncertainty (Herrera et al., 2022), and a trade-off between benefits of increased model
925 complexity and increased simulation uncertainty will result (Schilling et al., 2019). Simple
926 explicit modeling of water extraction for irrigation (e.g., channel-to-cropland transfers) could
927 alleviate trade-offs observed in this study. Conventional calibration metrics like NSE or KGE
928 could hamper the exploration of accurate catchment processes, as single statistical performance
929 measures are unable to capture all features of observed variables (Gupta et al., 1998). Seasonal
930 isotope observations increased bias sensitivity and skewed performance assessments under the
931 present metrics. Metrics underscoring seasonal variability could be more indicative on runoff
932 generation processes. In order to capture observations at different temporal scales, wavelet-
933 based objectives could be alternative in this context (Manikanta and Vema, 2022). In addition,
934 anthropogenic activities (e.g., water withdrawn mainly occurred during spring and summer)
935 were intensively implemented in specific seasons and not in others. Using metrics which
936 weaken the influences of these epistemic errors in the observed streamflow could be a potential
937 way to derive more correct parameter sets. In this regard, the limits of acceptability method,
938 defining lower and upper boundaries as the tolerance of simulations deviations, is potentially
939 useful in such heavily managed catchments (Beven, 2006), although setting the limits is still
940 challenging due to the lack of specific information of many management interventions (Wu et
941 al., 2025).

942
943
944
945
946
947
948
949
950
951
952
953
954
955
956
957
958
959
960
961
962
963
964
965
966

~~Despite having limited streamwater isotope samples due to the large scale of the sampled area, they were sufficient and actually very valuable to reveal some significant difference between catchments. This helped to better understand ecohydrological processes and to identify processes that were not adequately captured, such as some of the anthropogenic impacts discussed above. Isotope data at finer temporal resolution could help to better constrain ET partitioning processes in heavily modified catchments, as they certainly do in more natural environments (Soulsby et al., 2015). In addition, precipitation isotopes were from a global data product (Bowen and Revenaugh, 2003). The use of interannually averaged monthly values likely failed to capture short-term climate variability or anthropogenic influences (e.g., fossil fuel derived vapor), introducing errors in water source apportionment (e.g., hydrograph separation) (Xia et al., 2024; Yang and Yoshimura, 2024). Again, high resolution local data would be advantageous for such investigations.~~

However, sparse records of withdrawal volumes, associated irrigation patterns and potential unauthorized practices, as well as political sensitivities in data sharing may limit practical modelling.

Despite having relatively limited streamwater isotope samples compared to some other studies, their availability was invaluable for this intercomparison and revealed some significant difference between catchment function (Figure 3). Since the evaluation of trade-offs between discharge and isotopes primarily relied on the seasonal patterns of isotopes, the three years of seasonally sampled isotopes used for calibration and the monthly rainfall isotope inputs provide a sufficient basis for evaluation for the trade-offs. In addition, the potential anthropogenic impacts noted above were identified through the comparisons among the four catchments in the same region, further supporting the value of the analysis. This evaluation of trade-offs

967 between discharge and isotopes helped identify potential processes not adequately captured
968 through discharge alone in such a heavily managed catchment.

970 **5 Conclusions**

971 Stable water isotopes are valuable tracers ~~in tracking hydrological flow paths and for~~ identifying
972 water sources, offering the potential to constrain ~~equifinality in~~ ecohydrological models. While
973 model calibration in natural catchments typically exhibits slight trade-offs between isotopic
974 signatures and conventional hydrological variables (~~e.g., usually~~ discharge), this study
975 advances a novel perspective on the benefits and challenges of integrating isotopes in
976 catchments heavily ~~human-~~impacted catchments by human activities. Using the conceptual-
977 based, fully-distributed TAM in the STARR model, we calibrated both isotopes and streamflow
978 without explicitly parameterizing anthropogenic disturbances to investigate three critical issues:
979 (1) the ~~influence of human interventions on model performance,~~ (2) the potential of using
980 discharge alone in calibration to mislead process interrelations from simulations under
981 anthropogenic stress, and (3) the adaptability and value of seasonally sampled isotopes in such
982 contexts, and (3) the likely impacts of human interventions on model performance. We studied
983 four sub-catchments of the Middle Spree (Berste, Wudritz, Vetschauer, and Dobra), subjected
984 to contrasting anthropogenic pressures (long-term mining impacts, seasonal water
985 withdrawals), and derived Pareto-optimal solutions to help disentangle the additional insights
986 provided by isotope-aided calibration compared with streamflow alone.

987 The results demonstrate that ~~strong trade-offs between isotopes and streamflow in calibrations~~
988 ~~arise in such anthropogenically impacted catchments, where unquantified epistemic errors in~~
989 ~~streamflow observations caused by human activities compromise model reliability. Notably,~~
990 discharge-only based calibrations could mis-represent runoff partitioning processes, especially

991 in catchments with water withdrawals for irrigation, while isotopes helped identify implausible
992 simulations by being more realistic/informative on process representation. ~~The four study~~
993 ~~catchments were ET dominated, and~~ For example, higher groundwater contributions ~~to runoff~~
994 ~~were site specific. For example, Vetschauer displayed the most dynamic vertical fluxes, with~~
995 ~~groundwater storage fluctuations similar to soil storage in magnitude in the water balance,~~
996 ~~while Wudritz and Dobra showed minor groundwater contributions, consistent with the long-~~
997 ~~term mining effects. Isotope fractionation was very sensitive to the proportion of surface water~~
998 ~~area, and the absence of parameterising intermittent restored mining lakes in catchments~~
999 ~~resulted in worse results in ET partitioning processes. Further, isotopes help~~ were identified
1000 through isotope-aided calibrations. Isotopes also helped to disentangle ET partitioning, ~~even if~~
1001 ~~strong~~ although seasonally sampled isotopes could underestimate seasonally aggregated
1002 fractionations, and the absence of explicitly parameterizing the hydrology of small mining
1003 lakes could potentially mislead the results. Strong trade-offs in calibrations between isotopes
1004 and streamflow and isotopes occurred in calibrations arise in such anthropogenically-impacted
1005 catchments, where unquantified epistemic errors in streamflow observations caused by human
1006 activities can compromise model reliability.

1007 This study highlights how unaccounted anthropogenic activities can alter model interpretations
1008 and underscores the complementary role of isotopes and TAMs in refining simulations under
1009 complex human-environment interactions, although only seasonally sampled isotopes were
1010 employed. While distinct trade-offs between streamflow and isotopes were observed in the
1011 study catchments, ~~with Pareto-optimal solutions (e.g., Berste) failing to meet acceptable~~
1012 ~~performance thresholds,~~ these simulations still offer informative insights into ecohydrological
1013 dynamics and partitioning in heavily impacted catchments, even when quantitative process
1014 evaluation remains challenging. In catchments subject to intensive anthropogenic interventions
1015 (e.g., altered water distribution via irrigation or withdrawals), the severity of streamflow-

1016 isotope conflicts and compromises in TAM may serve as an indirect diagnostic of human
1017 impacts on water partitioning. Representing anthropogenic effects in ecohydrological models
1018 is inherently difficult, particularly when historical data on water use or management practices
1019 are sparse. However, we demonstrated here that TAMs ~~are still very~~ have valuable potential in
1020 such applications and encourage greater isotope sampling in anthropogenically influenced
1021 catchments.

1022

1023 **Acknowledgement**

1024 Hanwu Zheng is funded by the Chinese Scholarship Council (CSC). Tetzlaff's contribution was partly funded
1025 through the Einstein Research Unit "Climate and Water under Change" from the Einstein Foundation Berlin and
1026 Berlin University Alliance (grant no. ERU-2020- 609) and through the WETSCAPES2.0 project (DFG TRR410/1
1027 2025-), and Wasserressourcenpreis 2024 "of the Rüdiger Kurt Bode-Foundation". This research was (co-)funded
1028 by the Deutsche Forschungsgemeinschaft (DFG, German Research Foundation) – Transregio Collaborative
1029 Research Centre 410 "WETSCAPES2.0" (DFG TRR410/1 2025). Birkel's contribution was supported by a senior
1030 research fellowship of IGB and a sabbatical license by UCR. Contributions from Soulsby were supported by the
1031 Leibnitz Association Germany in the project Wetland Restoration in Peatlands and Mosaic II funded by Einstein
1032 Foundation. We are very grateful to Franziska Schmidt from the IGB Isotope Lab for the isotope analysis and
1033 colleagues from the Chemical Analytics and Biogeochemistry Lab of IGB for the isotope sampling. We are
1034 grateful to three anonymous reviewers whose constructive criticism of an earlier version of the manuscript greatly
1035 helped in strengthening the study.

1036 **Reference:**

- 1037 Ala-Aho, P., Tetzlaff, D., McNamara, J.P., Laudon, H., Soulsby, C., ~~2017~~2017a. Using
1038 isotopes to constrain water flux and age estimates in snow-influenced catchments using
1039 the STARR (Spatially distributed Tracer-Aided Rainfall-Runoff) model. *Hydrol. Earth
1040 Syst. Sci.* 21, 5089–5110. [https://doi.org/10.5194/hess-21-5089-](https://doi.org/10.5194/hess-21-5089-2017)
1041 ~~2017~~<https://doi.org/10.5194/hess-21-5089-2017>
- 1042 [Ala-aho, P. Tetzlaff, D., Wang, H. and Soulsby, C. 2017b. Integrated surface-subsurface models](#)
1043 [to investigate the role of groundwater in runoff generation in headwater catchments: a](#)
1044 [minimalist approach to parameterization. Journal of Hydrology.](#)
1045 [10.1016/j.hydrol.2017.02.023.](#)
- 1046 Arndt, S., Heiland, S., 2024. Current status of water-related planning for climate change
1047 adaptation in the Spree River basin, Germany. <https://doi.org/10.5194/nhess-2024-59>
- 1048 Beven, K., 2006. A manifesto for the equifinality thesis. *J. Hydrol.* 320, 18–36.
1049 <https://doi.org/10.1016/j.jhydrol.2005.07.007>
- 1050 Birkel, C., Soulsby, C., 2015. Advancing tracer-aided rainfall-runoff modelling: A review of
1051 progress, problems and unrealised potential. *Hydrol. Process.* 29, 5227–5240.
1052 <https://doi.org/10.1002/hyp.10594>
- 1053 Birkel, C., Soulsby, C., Tetzlaff, D., 2011. Modelling catchment-scale water storage dynamics:
1054 Reconciling dynamic storage with tracer-inferred passive storage. *Hydrol. Process.* 25,
1055 3924–3936. <https://doi.org/10.1002/hyp.8201>
- 1056 Blank, J., Deb, K., 2020. Pymoo: Multi-Objective Optimization in Python. *IEEE Access* 8,
1057 89497–89509. <https://doi.org/10.1109/ACCESS.2020.2990567>
- 1058 ~~Bowen, G.J., Revenaugh, J., 2003. Interpolating the isotopic composition of modern meteoric~~
1059 ~~precipitation. *Water Resour. Res.* 39, 1–13. <https://doi.org/10.1029/2003WR002086>~~
- 1060 [Bowen G. J., Wassenaar L. I. and Hobson K. A. \(2005\) Global application of stable hydrogen](#)

1061 [and oxygen isotopes to wildlife forensics. *Oecologia* 143, 337-348, doi:10.1007/s00442-](#)
1062 [004-1813-y.](#)

1063 Cao, R., Huang, H., Wu, G., Han, D., Jiang, Z., Di, K., Hu, Z., 2022. Spatiotemporal variations
1064 in the ratio of transpiration to evapotranspiration and its controlling factors across
1065 terrestrial biomes. *Agric. For. Meteorol.* 321, 108984.
1066 <https://doi.org/10.1016/j.agrformet.2022.108984>

1067 Chakraborty, S., Belekar, A.R., Datye, A., Sinha, N., 2018. Isotopic study of intraseasonal
1068 variations of plant transpiration: An alternative means to characterise the dry phases of
1069 monsoon. *Sci. Rep.* 8, 1–11. <https://doi.org/10.1038/s41598-018-26965-6>

1070 Chen, K., Tetzlaff, D., Goldhammer, T., Freymueller, J., Wu, S., Andrew Smith, A., Schmidt,
1071 A., Liu, G., Venohr, M., Soulsby, C., 2023. Synoptic water isotope surveys to understand
1072 the hydrology of large intensively managed catchments. *J. Hydrol.* 623, 129817.
1073 <https://doi.org/10.1016/j.jhydrol.2023.129817>

1074 Chow, V. Te, 1959. *Open-channel hydraulics*, Erlangga: Bandung. McGraw-Hill civil
1075 engineering series Civil.

1076 Correa, A., Birkel, C., Gutierrez, J., Dehaspe, J., Durán-Quesada, A.M., Soulsby, C., Sánchez-
1077 Murillo, R., 2020. Modelling non-stationary water ages in a tropical rainforest: A
1078 preliminary spatially distributed assessment. *Hydrol. Process.* 34, 4776–4793.
1079 <https://doi.org/10.1002/hyp.13925>

1080 Craig, H., Gordon, L.I., 1965. Isotopic oceanography: deuterium and oxygen-18 variation in
1081 the ocean and the marine atmosphere, in: *Stable Isotopes in Oceanographic Studies and*
1082 *Paleotemperatures*. Laboratorio di Geologia Nucleare, Pisa.

1083 Deb, K., Pratap, A., Agarwal, S., Meyerivan, T., 2002. A fast and elitist multiobjective genetic
1084 algorithm: NSGA-II. *IEEE Trans. Evol. Comput.* 6, 182–197.
1085 <https://doi.org/10.1109/4235.996017>

1086 Dehaspe, J., Birkel, C., Tetzlaff, D., Sánchez-Murillo, R., Durán-Quesada, A.M., Soulsby, C.,
1087 2018. Spatially distributed tracer-aided modelling to explore water and isotope transport,
1088 storage and mixing in a pristine, humid tropical catchment. *Hydrol. Process.* 32, 3206–
1089 3224. <https://doi.org/10.1002/hyp.13258>

1090 Deutscher Wetterdienst (DWD), 2024. Daily station observations (temperature, pressure,
1091 precipitation, sunshine duration, etc.) for Germany. URL <https://cdc.dwd.de/portal/>
1092 (accessed 5.25.24).

1093 Efstratiadis, A., Koutsoyiannis, D., 2010. One decade of multi-objective calibration approaches
1094 in hydrological modelling : a review 6667. <https://doi.org/10.1080/02626660903526292>

1095 Fatichi, S., Vivoni, E.R., Ogden, F.L., Ivanov, V.Y., Mirus, B., Gochis, D., Downer, C.W.,
1096 Camporese, M., Davison, J.H., Ebel, B., Jones, N., Kim, J., Mascaro, G., Niswonger, R.,
1097 Restrepo, P., Rigon, R., Shen, C., Sulis, M., Tarboton, D., 2016. An overview of current
1098 applications, challenges, and future trends in distributed process-based models in
1099 hydrology. *J. Hydrol.* 537, 45–60. <https://doi.org/10.1016/j.jhydrol.2016.03.026>

1100 Fenicia, F., McDonnell, J.J., Savenije, H.H.G., 2008. Learning from model improvement: On
1101 the contribution of complementary data to process understanding. *Water Resour. Res.* 44,
1102 1–13. <https://doi.org/10.1029/2007WR006386>

1103 Gibson, J.J., Edwards, T.W.D., 2002. Regional water balance trends and evaporation-
1104 transpiration partitioning from a stable isotope survey of lakes in northern Canada. *Global*
1105 *Biogeochem. Cycles* 16, 10-1-10–14. <https://doi.org/10.1029/2001gb001839>

1106 Godsey, S. E., W. Aas, T. A. Clair, et al. 2010. “Generality of Fractal 1/f Scaling in Catchment
1107 Tracer Time Series, and Its Implications for Catchment Travel Time Distributions.”
1108 *Hydrological Processes* 24, no. 12: 1660–1671. <https://doi.org/10.1002/hyp.7677>.

1109 Guevara-Escobar, A., Gonzalez-Sosa, E., Ramos-Salinas, M., Hernandez-Delgado, G.D., 2007.
1110 Experimental analysis of drainage and water storage of litter layers. *Hydrol. Earth Syst.*

- 1111 Sci. 11, 1703–1716. <https://doi.org/10.5194/hess-11-1703-2007>
- 1112 Gupta, H.V., Sorooshian, S., Yapo, P.O., 1998. Toward improved calibration of hydrologic
1113 models: Multiple and noncommensurable measures of information. *Water Resour. Res.*
1114 34, 751–763. <https://doi.org/10.1029/97WR03495>.
- 1115 [Gupta, H. V., Kling, H., Yilmaz, K. K., & Martinez, G. F. \(2009\). Decomposition of the mean](#)
1116 [squared error and NSE performance criteria: Implications for improving hydrological](#)
1117 [modelling. Journal of Hydrology, 377\(1–2\), 80–91.](#)
1118 <https://doi.org/10.1016/j.jhydrol.2009.08.003>.
- 1119 Herrera, P.A., Marazueta, M.A., Hofmann, T., 2022. Parameter estimation and uncertainty
1120 analysis in hydrological modeling. *Wiley Interdiscip. Rev. Water* 9, 1–23.
1121 ~~<https://doi.org/10.1002/wat2.1569>~~<https://doi.org/10.1002/wat2.1569>
- 1122 ~~Hodson, T.O., 2022. Root-mean-square error (RMSE) or mean absolute error (MAE): when to~~
1123 ~~use them or not. *Geosci. Model Dev.* 15, 5481–5487. [https://doi.org/10.5194/gmd-15-](https://doi.org/10.5194/gmd-15-5481-2022)~~
1124 ~~[5481-2022](https://doi.org/10.5194/gmd-15-5481-2022)~~
- 1125 [He, Z., Unger-Shayesteh, K., Vorogushyn, S., Weise, S. M., Kalashnikova, O., Gafurov, A.,](#)
1126 [Duethmann, D., Barandun, M., & Merz, B. \(2019\). Constraining hydrological model](#)
1127 [parameters using water isotopic compositions in a glacierized basin, Central Asia. *Journal*](#)
1128 [of Hydrology, 571, 332–348. <https://doi.org/10.1016/j.jhydrol.2019.01.048>](#)
- 1129 Holmes, T., Stadnyk, T.A., Kim, S.J., Asadzadeh, M., 2020. Regional Calibration With Isotope
1130 Tracers Using a Spatially Distributed Model : A Comparison of Methods. *Water Resour.*
1131 *Res.* 56. <https://doi.org/10.1029/2020WR027447>
- 1132 [Holmes, T. L., Stadnyk, T. A., Asadzadeh, M., & Gibson, J. J. \(2023\). Guidance on large scale](#)
1133 [hydrologic model calibration with isotope tracers. *Journal of Hydrology*, 621.](#)
1134 <https://doi.org/10.1016/j.jhydrol.2023.129604>
- 1135 Hrachowitz, M., Savenije, H.H.G., Blöschl, G., McDonnell, J.J., Sivapalan, M., Pomeroy, J.W.,

1136 Arheimer, B., Blume, T., Clark, M.P., Ehret, U., Fenicia, F., Freer, J.E., Gelfan, A., Gupta,
1137 H. V., Hughes, D.A., Hut, R.W., Montanari, A., Pande, S., Tetzlaff, D., Troch, P.A.,
1138 Uhlenbrook, S., Wagener, T., Winsemius, H.C., Woods, R.A., Zehe, E., Cudennec, C.,
1139 2013. A decade of Predictions in Ungauged Basins (PUB)-a review. *Hydrol. Sci. J.* 58,
1140 1198–1255. <https://doi.org/10.1080/02626667.2013.803183>

1141 Iorgulescu, I., Beven, K.J., Musy, A., 2007. Flow, mixing, and displacement in using a data-
1142 based hydrochemical model to predict conservative tracer data. *Water Resour. Res.* 43, 1–
1143 12. <https://doi.org/10.1029/2005WR004019>

1144 [J. Landgraf, D. Tetzlaff, M. Dubbert, D. Dubbert, A. Smith, C. Soulsby. Xylem water in](#)
1145 [riparian willow trees \(Salix alba\) reveals shallow sources of root water uptake by in situ](#)
1146 [monitoring of stable water isotopes. *Hydrol. Earth Syst. Sci.*, 26 \(2022\), pp. 2073-2092,](#)
1147 [10.5194/hess-26-2073-2022](#)

1148 Jung, H., Tetzlaff, D., Birkel, C., Soulsby, C., 2025. Recent Developments and Emerging
1149 Challenges in Tracer-Aided Modeling. *WIREs Water* 12.
1150 <https://doi.org/10.1002/wat2.70015>

1151 Karssenberg, D., Schmitz, O., Salamon, P., de Jong, K., Bierkens, M.F.P., 2010. A software
1152 framework for construction of process-based stochastic spatio-temporal models and data
1153 assimilation. *Environ. Model. Softw.* 25, 489–502.
1154 <https://doi.org/10.1016/j.envsoft.2009.10.004>

1155 Kirchner, J.W., 2006. Getting the right answers for the right reasons: Linking measurements,
1156 analyses, and models to advance the science of hydrology. *Water Resour. Res.* 42, 1–5.
1157 <https://doi.org/10.1029/2005WR004362>

1158 Kirchner, J.W., 2003. A double paradox in catchment hydrology and geochemistry. *Hydrol.*
1159 *Process.* 17, 871–874. <https://doi.org/10.1002/hyp.5108>

1160 Klaus, J., McDonnell, J.J., 2013. Hydrograph separation using stable isotopes: Review and

1161 evaluation. *J. Hydrol.* 505, 47–64. <https://doi.org/10.1016/j.jhydrol.2013.09.006>

1162 Kröcher, J., Ghazaryan, G., Lischeid, G., 2025. Unravelling Regional Water Balance Dynamics
1163 in Anthropogenically Shaped Lowlands: A Data-Driven Approach. *Hydrol. Process.* 39,
1164 1–17. <https://doi.org/10.1002/hyp.70053>

1165 Kuppel, S., Tetzlaff, D., Maneta, M.P., Soulsby, C., 2018. What can we learn from multi-data
1166 calibration of a process-based ecohydrological model? *Environ. Model. Softw.* 101, 301–
1167 316. <https://doi.org/10.1016/j.envsoft.2018.01.001>

1168 Landesregierung Brandenburg, 2024. Landesamt für Umwelt Brandenburg (LfU). URL
1169 <https://lfu.brandenburg.de/lfu/de/> (accessed 5.25.24).

1170 Landgraf, J., Tetzlaff, D., Birkel, C., Stevenson, J.L., Soulsby, C., 2023. Assessing land use
1171 effects on ecohydrological partitioning in the critical zone through isotope-aided
1172 modelling. *Earth Surf. Process. Landforms* 48, 3199–3219.
1173 <https://doi.org/10.1002/esp.5691><https://doi.org/10.1002/esp.5691>

1174 [J. Landgraf, D. Tetzlaff, S. Wu, J. Freymüller, C. Soulsby, 2022. Using stable water isotopes](#)
1175 [to understand ecohydrological partitioning under contrasting land uses in a drought-](#)
1176 [sensitive rural Lowland Catchment, pp. 1-41. https://doi.org/10.1002/hyp.14779](#)

1177 Lindström, G., Johansson, B., Persson, M., Gardelin, M., Bergström, S., 1997. Development
1178 and test of the distributed HBV-96 hydrological model. *J. Hydrol.* 201, 272–288.
1179 [https://doi.org/10.1016/S0022-1694\(97\)00041-3](https://doi.org/10.1016/S0022-1694(97)00041-3)

1180 Liu, J., Liu, X., Wang, Y., Li, Y., Jiang, Y., Fu, Y., Wu, Y.J.Á.Y.F.Á.J., 2020. Landscape
1181 composition or configuration : which contributes more to catchment hydrological flows
1182 and variations? *Landsc. Ecol.* 35, 1531–1551. <https://doi.org/10.1007/s10980-020->
1183 [01035-3](https://doi.org/10.1007/s10980-020-01035-3)

1184 Luo, S., Tetzlaff, D., Smith, A., Soulsby, C., 2024. Assessing impacts of alternative land use
1185 strategies on water partitioning, storage and ages in drought-sensitive lowland catchments

1186 using tracer-aided ecohydrological modelling. *Hydrol. Process.* 38, 1–21.
1187 <https://doi.org/10.1002/hyp.15126>

1188 Manikanta, V., Vema, V.K., 2022. Formulation of Wavelet Based Multi-Scale Multi-Objective
1189 Performance Evaluation (WMMPE) Metric for Improved Calibration of Hydrological
1190 Models. *Water Resour. Res.* 58, 1–20. <https://doi.org/10.1029/2020WR029355>

1191 Marx, C., Tetzlaff, D., Hinkelmann, R., Soulsby, C., 2021. Isotope hydrology and water
1192 sources in a heavily urbanized stream. *Hydrol. Process.* 35, 1–20.
1193 <https://doi.org/10.1002/hyp.14377>

1194 McDonnell, J.J., Beven, K., 2014. Debates - The future of hydrological sciences: A (common)
1195 path forward? A call to action aimed at understanding velocities, celerities and residence
1196 time distributions of the headwater hydrograph. *Water Resour. Res.* 50, 5342–5350.
1197 <https://doi.org/10.1002/2013WR015141>

1198 McDonnell, J.J., Sivapalan, M., Vaché, K., Dunn, S., Grant, G., Haggerty, R., Hinz, C., Hooper,
1199 R., Kirchner, J., Roderick, M.L., Selker, J., Weiler, M., 2007. Moving beyond
1200 heterogeneity and process complexity: A new vision for watershed hydrology. *Water*
1201 *Resour. Res.* 43, 1–6. <https://doi.org/10.1029/2006WR005467>

1202 Morris, M.D., 1991. Factorial sampling plans for preliminary computational experiments.
1203 *Technometrics* 33, 161–174.

1204 [Nan, Y., & Tian, F. \(2024\). Isotope data-constrained hydrological model improves soil](#)
1205 [moisture simulation and runoff source apportionment. *Journal of Hydrology*, 633.](#)
1206 <https://doi.org/10.1016/j.jhydrol.2024.131006>

1207 Oerter, E.J., Bowen, G.J., 2019. Spatio-temporal heterogeneity in soil water stable isotopic
1208 composition and its ecohydrologic implications in semiarid ecosystems. *Hydrol. Process.*
1209 33, 1724–1738. <https://doi.org/10.1002/hyp.13434>

1210 Oliveira, A.M., Fleischmann, A.S., Paiva, R.C.D., 2021a. On the contribution of remote

1211 sensing-based calibration to model hydrological and hydraulic processes in tropical
1212 regions. *J. Hydrol.* 597, 126184. <https://doi.org/10.1016/j.jhydrol.2021.126184>

1213 Paul-Limoges, E., Revill, A., Maier, R., Buchmann, N., Damm, A., 2022. Insights for the
1214 Partitioning of Ecosystem Evaporation and Transpiration in Short-Statured Croplands. *J.*
1215 *Geophys. Res. Biogeosciences* 127, 1–19. <https://doi.org/10.1029/2021JG006760>

1216 Pianosi, F., Sarrazin, F., Wagener, T., 2015. A Matlab toolbox for Global Sensitivity Analysis.
1217 *Environ. Model. Softw.* 70, 80–85. <https://doi.org/10.1016/j.envsoft.2015.04.009>

1218 Pohle, I., Koch, H., Grünewald, U., 2012. Potential climate change impacts on the water
1219 balance of subcatchments of the River Spree, Germany. *Adv. Geosci.* 32, 49–53.
1220 <https://doi.org/10.5194/adgeo-32-49-2012><https://doi.org/10.5194/adgeo-32-49-2012>

1221 [Pohle, I., Zeilfelder, S., Birner, J., and Creutzfeldt, B., 2025. The 2018–2023 drought in Berlin:
1222 impacts and analysis of the perspective of water resources management, *Nat. Hazards
1223 Earth Syst. Sci.*, 25, 1293–1313, <https://doi.org/10.5194/nhess-25-1293-2025>.](#)

1224 Pusch, M., Andersen, H.E., Behrendt, H., Tor, M., Hoffmann, C.C., Kronvang, B., Pedersen,
1225 M.L., Tor, M., Wolter, C., 2009. Rivers of the Central European Highlands and Plains
1226 525–576. <https://doi.org/10.1016/B978-0-12-369449-2.00014-X>

1227 Pusch, M., Hoffmann, A., 2000. Conservation concept for a river ecosystem (River Spree,
1228 Germany) impacted by flow abstraction in a large post-mining area. *Landsc. Urban Plan.*
1229 51, 165–176. [https://doi.org/10.1016/S0169-2046\(00\)00107-9](https://doi.org/10.1016/S0169-2046(00)00107-9)

1230 Rutter, A.J., Kershaw, K.A., Robins, P.C., Morton, A.J., 1972. A predictive Model of Rainfall
1231 Interception in Forests. *Agric. Meteorol.* 9, 367–384.

1232 [Schilling, O. S., Cook, P. G., & Brunner, P. \(2019\). Beyond classical observations in
1233 hydrogeology: The advantages of including exchange flux, temperature, tracer
1234 concentration, residence time and soil moisture observations in groundwater model
1235 calibration. *Rev. Geophys.*, 57\(1\), 146-182. <https://doi.org/10.1029/2018RG000619>](#)

- 1236 Schlesinger, W.H., Jasechko, S., 2014. Transpiration in the global water cycle. *Agric. For.*
1237 *Meteorol.* 189–190, 115–117. <https://doi.org/10.1016/j.agrformet.2014.01.011>
- 1238 Scudeler, C., Pangle, L., Pasetto, D., Niu, G.Y., Volkmann, T., Paniconi, C., Putti, M., Troch,
1239 P., 2016. Multiresponse modeling of variably saturated flow and isotope tracer transport
1240 for a hillslope experiment at the Landscape Evolution Observatory. *Hydrol. Earth Syst.*
1241 *Sci.* 20, 4061–4078. <https://doi.org/10.5194/hess-20-4061-2016>
- 1242 Seibert, J., Vis, M.J.P., 2012. Teaching hydrological modeling with a user-friendly catchment-
1243 runoff-model software package. *Hydrol. Earth Syst. Sci.* 16, 3315–3325.
1244 <https://doi.org/10.5194/hess-16-3315-2012>
- 1245 Shah, S., Duan, Z., Song, X., Li, R., Mao, H., Liu, J., Ma, T., Wang, M., 2021. Evaluating the
1246 added value of multi-variable calibration of SWAT with remotely sensed
1247 evapotranspiration data for improving hydrological modeling. *J. Hydrol.* 603, 127046.
1248 <https://doi.org/10.1016/j.jhydrol.2021.127046>
- 1249 Shen, H., Tolson, B.A., Mai, J., 2022. Time to Update the Split-Sample Approach in
1250 Hydrological Model Calibration. *Water Resour. Res.* 58, 1–26.
1251 <https://doi.org/10.1029/2021WR031523>
- 1252 Simůnek, J., Sejna, M., Saito, H., van Genuchten, M.T., 2013. The HYDRUS-1D Software
1253 Package for Simulating the One-Dimensional Movement of Water, Heat, and Multiple
1254 Solutes in Variably-Saturated Media. *Dep. Environ. Sci. Calif. RIVERSIDERIVERSIDE,*
1255 *Calif.*
- 1256 Smith, A., Tetzlaff, D., Kleine, L., Maneta, M., Soulsby, C., 2021. Quantifying the effects of
1257 land use and model scale on water partitioning and water ages using tracer-aided
1258 ecohydrological models. *Hydrol. Earth Syst. Sci.* 25, 2239–2259.
1259 <https://doi.org/10.5194/hess-25-2239-2021>
- 1260 Smith, A.A., Tetzlaff, D., Maneta, M., Soulsby, C., 2022. Critical Zone Response Times and

1261 Water Age Relationships Under Variable Catchment Wetness States: Insights Using a
1262 Tracer-Aided Ecohydrological Model. *Water Resour. Res.* 58.
1263 <https://doi.org/10.1029/2021WR030584>

1264 Soulsby, C., Birkel, C., Geris, J., Dick, J., Tunaley, C., Tetzlaff, D., 2015. Stream water age
1265 distributions controlled by storage dynamics and nonlinear hydrologic connectivity:
1266 Modeling with high-resolution isotope data. *Water Resour. Res.* 51, 7759–7776.
1267 <https://doi.org/10.1002/2015WR017888>

1268 Sprenger, M., Tetzlaff, D., Soulsby, C., 2017. Soil water stable isotopes reveal evaporation
1269 dynamics at the soil-plant-atmosphere interface of the critical zone. *Hydrol. Earth Syst.*
1270 *Sci.* 21, 3839–3856. <https://doi.org/10.5194/hess-21-3839-2017>

1271 Sprenger, M., Volkmann, T.H.M., Blume, T., Weiler, M., 2015. Estimating flow and transport
1272 parameters in the unsaturated zone 2617–2635. [https://doi.org/10.5194/hess-19-2617-](https://doi.org/10.5194/hess-19-2617-2015)
1273 [2015](https://doi.org/10.5194/hess-19-2617-2015)

1274 Stevenson, J.L., Birkel, C., Comte, J.C., Tetzlaff, D., Marx, C., Neill, A., Maneta, M., Boll, J.,
1275 Soulsby, C., 2023. Quantifying heterogeneity in ecohydrological partitioning in urban
1276 green spaces through the integration of empirical and modelling approaches. *Environ.*
1277 *Monit. Assess.* 195. <https://doi.org/10.1007/s10661-023-11055-6>

1278 Sun, W., Wang, Y., Wang, G., Cui, X., Yu, J., Zuo, D., Xu, Z., 2017. Physically based
1279 distributed hydrological model calibration based on a short period of streamflow data:
1280 case studies in four Chinese basins. *Hydrol. Earth Syst. Sci.* 21, 251–265.
1281 <https://doi.org/10.5194/hess-21-251-2017><https://doi.org/10.5194/hess-21-251-2017>

1282 [Tafvizi, A., James, A. L., Holmes, T., Stadnyk, T., Yao, H., & Ramcharan, C. \(2024\).](https://doi.org/10.1016/j.jhydrol.2024.131377)
1283 [Evaluating the significance of wetland representation in isotope-enabled distributed](https://doi.org/10.1016/j.jhydrol.2024.131377)
1284 [hydrologic modeling in mesoscale Precambrian shield watersheds. *Journal of Hydrology,*](https://doi.org/10.1016/j.jhydrol.2024.131377)
1285 [637, 131377. <https://doi.org/10.1016/j.jhydrol.2024.131377>](https://doi.org/10.1016/j.jhydrol.2024.131377)

1286 [Tunaley, C., Tetzlaff, D., Birkel, C., & Soulsby, C. \(2017\). Using high-resolution isotope data](#)
1287 [and alternative calibration strategies for a tracer-aided runoff model in a nested catchment.](#)
1288 [Hydrological Processes, 31\(22\), 3962–3978. <https://doi.org/10.1002/hyp.11313>](#)

1289 van der Sande, C.J., de Jong, S.M., de Roo, A.P.J., 2003. A segmentation and classification
1290 approach of IKONOS-2 imagery for land cover mapping to assist flood risk and flood
1291 damage assessment. *Int. J. Appl. Earth Obs. Geoinf.* 4, 217–229.
1292 [https://doi.org/10.1016/S0303-2434\(03\)00003-5](https://doi.org/10.1016/S0303-2434(03)00003-5)

1293 van Huijgevoort, M.H.J., Tetzlaff, D., Sutanudjaja, E.H., Soulsby, C., 2016. Using high
1294 resolution tracer data to constrain water storage, flux and age estimates in a spatially
1295 distributed rainfall-runoff model. *Hydrol. Process.* 30, 4761–4778.
1296 <https://doi.org/10.1002/hyp.10902>

1297 Von Hoyningen-Huene, J., 1981. Die Interzeption des Niederschlages in landwirtschaftlichen
1298 Pflanzenbeständen. *Arbeitsbericht Deutscher Verband fuer Wasserwirtschaft und*
1299 *Kulturbau, Schriftenr. dtsh. verb. wasserwirtsch. kulturbau, hamburg berlin. DVWK,*
1300 *Braunschweig, Germany. https://doi.org/10.1007/978-3-642-41714-6_91316*

1301 Wada, Y., Bierkens, M.F.P., De Roo, A., Dirmeyer, P.A., Famiglietti, J.S., Hanasaki, N., Konar,
1302 M., Liu, J., Schmied, H.M., Oki, T., Pokhrel, Y., Sivapalan, M., Troy, T.J., Van Dijk,
1303 A.I.J.M., Van Emmerik, T., Van Huijgevoort, M.H.J., Van Lanen, H.A.J., Vörösmarty,
1304 C.J., Wanders, N., Wheeler, H., 2017. Human-water interface in hydrological modelling:
1305 Current status and future directions. *Hydrol. Earth Syst. Sci.* 21, 4169–4193.
1306 <https://doi.org/10.5194/hess-21-4169-2017>

1307 Wanders, N., Bierkens, M.F.P., de Jong, S.M., de Roo, A., Karssenber, D., 2014. The benefits
1308 of using remotely sensed soil moisture in parameter identification of large-scale
1309 hydrological models. *Water Resour. Res.* 50, 6874–6891.
1310 <https://doi.org/10.1002/2013WR014639>

1311 Wu, S., Tetzlaff, D., Beven, K., Soulsby, C., 2025. DREAM(LoAX): Simultaneous Calibration
1312 and Diagnosis for Tracer-Aided Ecohydrological Models Under the Equifinality Thesis.
1313 Water Resour. Res. 61. <https://doi.org/10.1029/2024WR038779>

1314 Wu, S., Tetzlaff, D., Yang, X., Smith, A., Soulsby, C., 2023. Integrating Tracers and Soft Data
1315 Into Multi-Criteria Calibration: Implications From Distributed Modeling in a Riparian
1316 Wetland. Water Resour. Res. 59, 1–21. <https://doi.org/10.1029/2023WR035509>

1317 Xia, C., Zuecco, G., Marchina, C., Penna, D., Borga, M., 2024. Effects of Short-Term Climate
1318 Variations on Young Water Fraction in a Small Pre-Alpine Catchment. Water Resour.
1319 Res. 60, 1–22. <https://doi.org/10.1029/2023WR036245>

1320 Yang, X., Tetzlaff, D., Müller, C., Knöller, K., Borchardt, D., Soulsby, C., 2023. Upscaling
1321 Tracer-Aided Ecohydrological Modeling to Larger Catchments: Implications for Process
1322 Representation and Heterogeneity in Landscape Organization. Water Resour. Res. 59.
1323 <https://doi.org/10.1029/2022WR033033>

1324 Yang, Y., Yoshimura, K., 2024. Simulation of Water Isotopes in Combustion-Derived Vapor
1325 Emissions in Winter. J. Geophys. Res. Atmos. 129.
1326 <https://doi.org/10.1029/2023JD040543><https://doi.org/10.1029/2023JD040543>

1327 [Ying, Z., D. Tetzlaff, J. Freymueller, J.-C. Comte, A. Schmidt, and C. Soulsby. 2024.](#)
1328 [“Developing a Conceptual Model of Groundwater – Surface Water Interactions in a](#)
1329 [Drought Sensitive Lowland Catchment Using Multi-Proxy Data.” Journal of Hydrology](#)
1330 [628: 130550. https://doi.org/10.1016/j.jhydrol.2023.130550](#)

1331 Zhang, Y., Kong, D., Gan, R., Chiew, F.H.S., McVicar, T.R., Zhang, Q., Yang, Y., 2019.
1332 Coupled estimation of 500 m and 8-day resolution global evapotranspiration and gross
1333 primary production in 2002–2017. Remote Sens. Environ. 222, 165–182.
1334 <https://doi.org/10.1016/j.rse.2018.12.031>

1335

1336
1337
1338
1339
1340
1341
1342
1343
1344
1345
1346
1347
1348
1349
1350
1351
1352
1353
1354
1355
1356
1357
1358
1359
1360
1361